Estimation of critical temperature of nano-confined alkanes using vapour-liquid interfacial free energy

A Dissertation

Submitted in the partial fulfillment of the requirements for the award of degree of

Masters of Sciences

In

Chemistry

Submitted By

Naincy Attri

(Roll No.301602029)

Under the Supervision of

Dr. Sudhir K Singh

(Associate Professor)

Department of Chemical Engineering

School of Chemistry and Biochemistry

Thapar Institute of Engineering and Technology

Patiala, 147004

June 2018

CERTIFICATE

This is to certify that the dissertation entitled "**Estimation of critical temperature of nano-confined alkanes using vapour-liquid interfacial free energy**" being submitted by Ms. Naincy Attri in partial fulfilment of the requirements for the award of degree of Master of Science in Chemistry and being submitted to the School of Chemistry and Biochemistry, Thapar Institute of Engineering and Technology, Patiala, is a bonafide work carried by her under our supervision. The work has reached the standard necessary for submission. The contents of this dissertation have not been submitted for the award of any other degree or diploma.

Sudhir Kr. Singh

Dr. Sudhir K.Singh
Associate Professor,
Department of Chemical Engineering,
TIET, Patiala -147004

CANDIDATE's DECLARATION

I hereby declare that the work being presented in the dissertation entitled "**Estimation of critical temperature of nano-confined alkanes using vapour-liquid interfacial free energy**" in partial fulfilment of the requirements for the award of degree of Masters of Science in Chemistry and being submitted to School of Chemistry and Biochemistry, Thapar institute of engineering and technology, Patiala, is my own work during the period of January to July 2017, under the supervision of **Dr. Sudhir K Singh**. I have not submitted embodied in this dissertation for the award of any other degree.

Patiala **Naincy Attri**

Date: 27/7/2018

This is certify that the above statement made by the candidate is correct and true to the best of our knowledge.

Sudhir Kr. Singh

Dr Sudhir K Singh
Associate Professor,
Department of Chemical Engineering,
TIET, Patiala-147004

ACKNOWLEDGEMENT

First of all, I owe my gratitude to the Head of the Department, **Dr. Amjad Ali** for providing me the opportunity in the form of this dissertation to develop my interest in research.

In the same spirit, I would like to thank my Supervisor, **Dr. Sudhir K Singh** for his constructive guidance and constant support during the project. The work presented here could not have been accomplished without their patience and ever willingness to teach. They have taught me to concise and correct in my approach from the formulation of ideas to the presentation of the results.

Special thanks to all the **Teaching Faculty** of the department for their cooperation and guidance.

I am grateful to **TIET & School of chemistry and biochemistry** for providing financial support and all necessary infrastructure and laboratory facilities to carry out the experimental work.

Words fail me to express my thanks to my family and friends who have always supported me and have been a source of strength and inspiration to me during the entire period of the work.

All the thanks are, however, only fraction of what is due to almighty for granting me an opportunity and strength to successfully accomplish this project.

Date: 27/7/2018 Naincy Attri

ABSTRACT

The critical temperature of bulk and confined alkanes are investigated making use of vapour-liquid interfacial free energy of coexistence received from grand-canonical transition matrix Monte Carlo simulations utilizing a histogram reweighting technique. For a system underneath investigation the temperature equivalent to zero interfacial free energy of coexistence is the estimated critical temperature. The acquired critical temperatures have revealed nonlinear monotonic tendency with converse of slit width. Moreover, four to five different linear regimes of critical temperature are observed in the studied series of slit width. In this work, Buckingham exponential-6 potential model is used to depict the interaction between alkane's molecules and Steele potential is used for the interaction between confining surface (Graphite/Mica) and alkane molecules. In this investigation methane, n-butane and n-octane are subjected under graphite and mica slit pores of varying slit width. In case of methane; graphite slit width varied from 40 Å to 5.4 Å and mica slit width varied from 40 Å to 5 Å, for n-butane; graphite slit width varied from 40 Å to 5.8 Å and mica slit width varied from 40 Å to 5.5 Å, for n-octane; graphite slit width varied from 50 Å to 7 Å and mica slit width varied from 50 Å to 6.5 Å. This investigation additionally reveals that the critical temperature of bulk and confined alkane estimated using the vapour-liquid interfacial free energy of coexistence is within logical accuracy with that obtained using the simplified form of scaling law.

Keywords: Critical temperature, Confined alkane, Interfacial free energy, Monte Carlo, Slit width

LIST OF CONTENTS

CHAPTER-1

INTRODUCTION

1.1 Critical Temperature

The critical temperature of a pure substance is that temperature at which vapour of the substance cannot be liquefied, regardless of what quantity pressure is applied. This is the highest temperature at that it possible to separate substances into two fluid phases (vapour and liquid). At critical temperature the difference between vapour and liquid phases disappear and vapour liquid interfacial free energy approaches to zero.

1.2 Confined fluid

Take any fluid in an exceedingly closed system. Confined fluids will move around among the system; however they can't enter or leave the system. Curbed to area or volume is called *confinement*. So, in an extremely large world, fluids confined by surrounding surfaces of any form or shape that are visible by the normal human are defined as confined fluids.

Reduction of the size of pattern of a substance to the nanometer scale endows it with properties and behaviour that absolutely unique from those of the bulk material. It's not simply the isolated nanosample of a material that has properties entirely specific from constant bulk material; interaction with the walls that confine a sample in an extremely small volume further alters its properties and behaviour. These changes in behaviour arise once the diverge of molecular interaction and therefore the length scale related to position correlation within the material which is same as the length scale of the confinement. It is usually found that fluids confined between two walls with small separation become ordered into layers that have lateral internal ordering moreover as transversal ordering between layers.

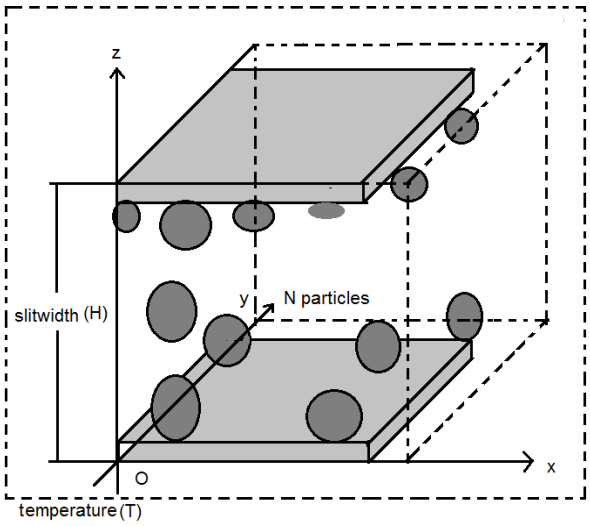

Figure 1.1 Nano confined fluid

1.3 Vapour-liquid Interfacial free energy

Interfacial free energy is that excess free energy related to an interface. This excess free energy is that energy value associated with the introduction of that interface.

Vapour-liquid phase equilibria of square well alkane of variable interaction range in hard slit pores are studied by means of grand-canonical transition-matrix Monte Carlo (GC-TMMC) simulation. Critical density under confinement shows oscillatory manners as slit width, ***H***, condensed from 12σ to 1σ. Two linear regimes are initiate for the slit in the critical temperature with the converse in the slit width. The first regime is seen for H>2.0σ with linear increase in the slope of shift in the critical temperature against inverse slit width with increasing interaction range. Consequent decrease in ***H*** has little effect on the critical temperature and it remains almost constant.

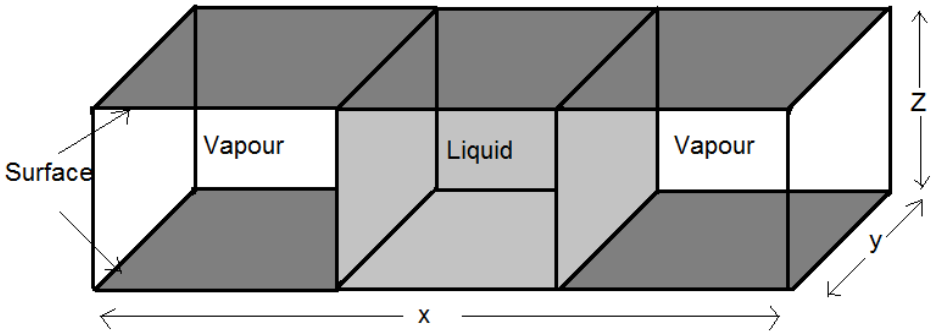

Figure 1.3 Diagram of simulation hot with vapour and liquid coexistence under slit pore confinement of slit width, ***H*** = z

1.4 Critical temperature estimation techniques

1) Fourth-order Binder's cumulant approach.
2) Simplified form of scaling law of density.
3) Mixed-field finite size scaling.
4) Using vapour-liquid interfacial free energy

1) Fourth-order Binder cumulant approach

Fourth-order Binder cumulant approach [1,2,3,4] used to calculate the critical temperature of bulk and confined square-well fluid in slit pore of two pore sizes. Further this come close to estimate the critical temperature of moderately more complex fluids such as n-alkanes confined in graphite and mica slit pores of different slit widths. The estimated critical temperatures are compared with critical temperature obtained for the similar system using simplified form of the scaling law[5]. This investigation reveals that critical temperatures of simple and confined alkane in bulk state and under confinement, estimated using scaling law, are contained by reasonable accuracy with that obtained using more accurate and precise approach of fourth-order Binder's cumulant.

2) Scaling law of density

i) Comprehensive study of scaling law of density by Wegner. Wegner[6] showed that away from the critical point, the difference in coexisting vapour and liquid densities can be written in the following form:

$$\rho_l - \rho_v = C_0\left(1-\frac{T}{T_c}\right)^{\beta} + C_1\left(1-\frac{T}{T_c}\right)^{\beta+\Delta} + C_2\left(1-\frac{T}{T_c}\right)^{\beta+2\Delta} + \ldots \qquad (1)$$

Where ρ_l, ρ_v and T_c are coexistence liquid and vapour number densities and critical temperature, respectively;

Δ is the gap exponent

Cj are the correction amplitude or coefficients.

The parameter ß is known as order parameter critical exponent.

ii) Simplified form of Scaling law of density

Further, using the following simplified from of Equation (1), Tc is estimated as

$$\rho_l - \rho_v = C_0 \left(1 - \frac{T}{T_c}\right)^{\beta} \qquad (2)$$

To our best knowledge, there is no literature report on the estimation of critical temperature using vapour-liquid interfacial free energy of finite size system and its similarity with the critical temperature obtained using simplified form of scaling law of density [7,5,8] represented in the form of Eq.(2).

3) Mixed-field Finite Size scaling

By matching the probability distribution of the ordering operator, p(M), to the three-dimensional (3D) and two dimensional (2D) using universality classes according to the mixed-field finite size scaling[9,10,11] approach, we create a ”phase diagram” in the(H,L) plane, screening the boundary between four types of behavior : 3D, quasi-3D,quasi-2D, and 2D. In order to assist 2D critical point calculation, we present a four parameter analytical expression for the 2D using universal distribution. We show that the infinite-system-size critical points obtained by extrapolation from the visible 3d and 2D critical points have only insignificant differences with each other. In contract with recent reports in the literature[Jana et al.., j. Chem. Phys. 130, 214707 (2009)], we find disappearance from linearity in the relationship between critical temperature and inverse wall separation, as well as nonmonotonic dependence of the critical density and the liquid density at coexistence upon wall separation. Further studies of the ST2 model of water show related behavior, which suggests that these are quite common properties of confined alkane.

4) Using vapour-liquid interfacial free energy

Vapour-liquid interfacial free energy technique used in current work.

1.5 Objective of current work

Objective of current work to study the critical temperature estimation of bulk and confined alkane using vapour-liquid interfacial free energy using molecular simulation techniques. We address, for the first time in detail, the degree of confinement on the critical temperature of confined alkanes. The basic scientific interest to identify the new physics behind the confined alkane that results from finite size effects, varying dimensionality and surface forces. Precisely we looked at the vapour-liquid interfacial free energy and critical properties. In our investigation, it has been observed that vapour-liquid critical temperature is concealed under confinement. In this work, for a given slit width, the free energy barrier between vapour and liquid phases at coexistence is estimated for a certain system size at various temperatures in an appropriate range. In this work, we have also compared the critical temperature estimation of bulk and confined alkane from two methods (i) simplified form of scaling law density[7.5,8] (ii) the critical temperature estimated by the fitting of vapour-liquid interfacial free energy of finite size system.

In this work, by performing careful computer experiments (computer simulations) using, (GC-TMMC) grand canonical transition matrix Monte Carlo simulation technique[7,5,12,13]. We investigated and compared the critical temperature estimation of bulk and confined alkanes using vapour-liquid interfacial free energy and the confinement of n-alkanes in mica and graphite slit pore of varying slit widths.

CHAPTER 2

Review of literature

Detailed understanding of the vapour-liquid phase coexistence and critical properties of bulk and confined alkane is of fundamental importance for the explanation of experimental data on fluids in nanopores [14,15,16]. A complete review on confined fluid is found in Gelb et al.[17]. The fundamental scientific interest on confined alkane is to understand the new physics that results from finite size effects, varying dimensionality and surface forces. Due to difficulties in conducting experimental studies on the characterization of atomistic behaviours, molecular simulation is used to conduit the theories and the experimental outcomes. Often, experimentally unexpected however promising paths to final products are originate by computational methods. The rapid increases in computer power and new efficient algorithms have further enhanced the use of computational methods, and have made very difficult problems solve. Vapour-liquid equilibrium and critical temperature of confined alkane have been studied by several investigators using experimental[18,19,20,21] theoretical[22] and molecular simulation approaches[23,24,25,26,27,28,29,30]. In these investigations, it has been observed that vapour-liquid critical temperature is concealed under confinement. Moreover, critical temperature of confined alkane depend on two major factors, (i) the range and strength of attractive and repulsive interactions and (ii) pore width of the system under investigation[7,5]. In an investigation using Monte Carlo simulation, Vishnyakov et al.[23] observed linear dependence of critical temperature of Lennard-Jones fluid on studied slit widths. On the other hand, later investigations of Vortler[24] and others[7,9] suggest nonlinear behaviour of critical temperature with respect to slit width as a more basic behaviour. Similarly nonlinear behaviour of critical temperature is observed with the square-well fluid confined in cylindrical pore of varying pore widths[31]. Significantly, in the vicinity of the critical point due to the finite size effects[32] the computer simulations cannot give correct results, which do not agree to talking into report the long range density fluctuations[33]. Hence, numerous methods have been devised to estimate the critical temperature on the basis of analysis of numerical data obtained from simulations. Major

method have been practical for bulk, confined and two dimensional fluids include mixed-field finite size scaling technique[9,10,11] simplified form of scaling law of density[7,5,8] and fourth-order Binder cumulant approach[1,4]. Moreover, it has been revealed in previous investigations that the rational intermolecular potentials, the arrangement of histogram reweighting techniques with Binder fourth-order cumulant calculation is completely equivalent to the mixed-field method and can be working in a finite system size study in order to estimate the critical parameters with the same accuracy as for the mixed-field studies [34].

To our best information, there is no literature report on estimation of critical temperature using vapour-liquid interfacial free energy of finite size system and its contrast with the critical temperature obtained using simplified form of scaling law[5]. In this work, for a given slit width, the free energy barrier between vapour and liquid phases at coexistence is estimated for a certain system size at various temperatures in an suitable range. The free energy data obtained are fixed with the second- degree polynomial to estimate the temperature corresponding to zero interfacial free energy. "The temperature corresponding to the zero interfacial free energy represents the estimated critical temperature". In this work, we have also compared the critical temperature estimation of bulk and confined alkane from two methods viz., simplified form of scaling law density[5] and the critical temperature estimated by the fitting of vapour-liquid interfacial free energy of finite size system.

In 2007, Hamada used grand canonical Monte Carlo numerical simulations to study thermodynamic properties of confined Lennard-Jones (LJ) particles in slit and cylindrical pore systems and indicated changes in fluid phase behavior as a purpose of pore radius. Singh (2009) investigated the behavior of methane (C1), n-butane (C4) and n-octane (C8) inside nanoscale slits with widths between 0.8 to 5 nm using grand canonical Monte Carlo simulations and establish out that while critical temperature decreased with decline in pore radius, the critical pressures of n-butane and n-octane first increased and consequently decreased. They also found that the critical property shift is reliant on pore surface types and hence differed for mica and graphite.

Understanding the behavior of alkanes under nanoconfinements is of enormous interest from fundamental and practical perspectives. In common, fluids less than any type of confinement within pores of nanometer size show major variation from bulk thermophysical and structural properties[35]. Such systems are in between bulk matter and single atoms or molecules, and as a result, finite size and surface effects become necessary for the investigation of such systems.

In addition, a fundamental understanding of the various thermophysical and interfacial phenomena, in the occurrence of surfaces, it is essential for many industrial and geometrical operations. For examples, micro and mesoporous materials are widely used in chemical, oil and gas, feed, and pharmaceutical industries for pollution control, mixture separation, and purification and as catalysts and catalyst supports for chemical reaction[14,36,16]. The propose of such processes is largely observed with an underdeveloped scientific basis because the theory-based perceptive of confined fluids is still not completely understood[37]. Capillary phase transitions and adsorption and partition properties of mixtures of n-alkanes in a carbon nanotube were studied using gauge-cell Monte Carlo simulation[38,39]. It was observed by the investigators that confinement of n-alkanes in a carbon nanotube decreases its critical temperature and increases its critical density.

Zhang[40] used molecular dynamics simulation techniques to study the density profiles, structural properties, and average diffusion coefficients of n-decane in a carbon nanotube. The author observed in density profiles the well-defined peaks, which indicated a strong affinity of layer creation in the nanotube. Further, the structural properties were originate to vary strappingly with the radial position of the chain's center of mass. In some recent work, single-component adsorption of methane, [41,42] ethane, [43,44,45] and some other higher n-alkanes[46,47] by the side of its adsorption isotherms and density and orientation profiles was investigated in carbon slit pores using Monte Carlo simulations. Furthermore, there have been several molecular dynamics simulations for chain molecules in slit pores. These molecular dynamics simulation were used to study the density profiles and chain

conformations of linear and branched alkanes under shear-flow conditions[14,48,49,50,51,52]. These investigations specify that there is a thoughtful influence of the slit surfaces on the fluid structure. However, in all of the above mentioned work, authors did not investigate thoroughly changes in the critical and vapor-liquid interfacial properties under confinement with changes in the pore width, particularly those imminent the two-dimensional limit. This is the major objective of the current work. In this work, we have investigated thermophysical properties of n-alkanes confined in graphite and mica slit pores. In particular, we present the phase coexistence properties (saturated density and vapor pressures), critical properties (critical temperature, pressure, and density), local density and orientation profiles of liquid and vapor phases, and interfacial properties (vapor-liquid surface tension) of n-alkanes of chain length C1-C8, with changes in the slit-width, temperature and surface characteristics.

In this work, we have investigated and compared the critical temperature estimation of bulk and confined alkane using vapour-liquid interfacial free energy, confined in mica and graphite slit pores of different slit widths. In the Chapter 3, we briefly explain the molecular simulation Methodology and techniques used to estimate critical temperature of bulk and confined alkane using vapour-liquid interfacial free energy

CHAPTER-3

3.1. Methodology

3.1.1. Introduction to Monte Carlo Simulations

Monte Carlo simulations may be defined as a set of methods in which the conformation and individual place of every molecule in the system is clearly accounted. In reward, molecular simulation can consider much larger systems, and this repeatedly makes it possible to develop visible macroscopic properties (i.e. that can be compared with measured experimental quantities) using microscopic information provided by the well-recognized framework of statistical thermodynamics. Monte Carlo methods are most appropriate for calculation by computer. In molecular simulations, Monte Carlo is approximately always used to turn to methods that use a technique called importance sampling. Importance sampling methods are capable to produce states of low energy, as this enables properties to be calculated correctly.

The Metropolis algorithm generates a Markov chain of states which satisfies the following two conditions:

a) The outcome of the each trial depends upon the preceding trial and not upon any previous trials.

b) Each trial belongs to a finite set of probable outcomes.

Monte Carlo simulation involves the repeated application of an elementary procedure as follows:

1. A trial configuration is generated by perturbing the original configuration of particles e.g. a randomly chosen atom is moved by small amount from its present position.
2. The ratio of probabilities, as per complete balance for the trial and creative configurations is computed, and from this amount a decision is made whether to accept or decline the trial.
3. If the trial is expected, the new configuration is taken as the next state in the Markov chain; otherwise the original configuration is taken as the next state in chain.

4. Standard properties of interest are composed over many independent configurations generated using the above steps.

The schematic of the above elementary procedure can be represented as shown in Figure 3.1.

Figure 3.1 Schematic of a Monte Carlo Simulation in the perspective of the canonical ensemble. Symbol X represents the average property such as E, V, P i.e. average energy, volume and pressure respectively.

Depending upon the ensemble used for the simulation method in general, Monte Carlo simulation is categorized into five classes:

1. NVE–MC: - It is micro canonical ensemble where number of volume, energy and particles are kept constant during simulation.

2. NVT–MC: - This canonical ensemble in which number of volume, temperature and particles are kept constant during the simulation.

3. NPT–MC: - It is isothermal–isobaric ensemble where number of particles, temperature and pressure are kept constant during the simulation.

4. GE–MC: - A particular case of Monte Carlo simulation in which interface energy is not accounted for. In this Gibbs ensemble, both temperature and the total number of particles are fixed, and we can impress either i.e. the sum of phase volumes or pressure.

5. mVT – MC: -This is also GCMC, grand canonical ensemble. Where chemical potential (m), volume and temperature are kept constant, while number of particles fluctuates during the simulation. This collection is most expedient statistical ensemble to simulate e.g. interfacial properties, adsorption isotherms; moreover of pure compounds or multi-component systems and gives a way to compare the experimental results explicitly. The basic idea in GCMC simulation is to replace the particles from a reservoir to sub system and vice versa keeping the chemical potential, m, constant. We imagine that the

molecules in the two sub volumes are actually identical particles. The only difference is that when they are in the volume V, they interact and when they are in the volume $V_0 - V$, they do not. The key feature about the GCMC method is that the number of particles may change during the simulation.

There are three basic moves in a GCMC simulation:

I) **Displacement Trial Move**:- A particle is displaced in the simulation box, using the common Metropolis method

II) **Deletion Trial Move**: - A particle is detached from the simulation box

III) **Insertion Move Trial**: - A particle is added at a random position in the simulation box. These basic moves are schematically shown in the Fig.3.2. Moreover, for chain molecules two more moves, rotation and regrowth of particle are integrated along with the above mentioned basic moves.

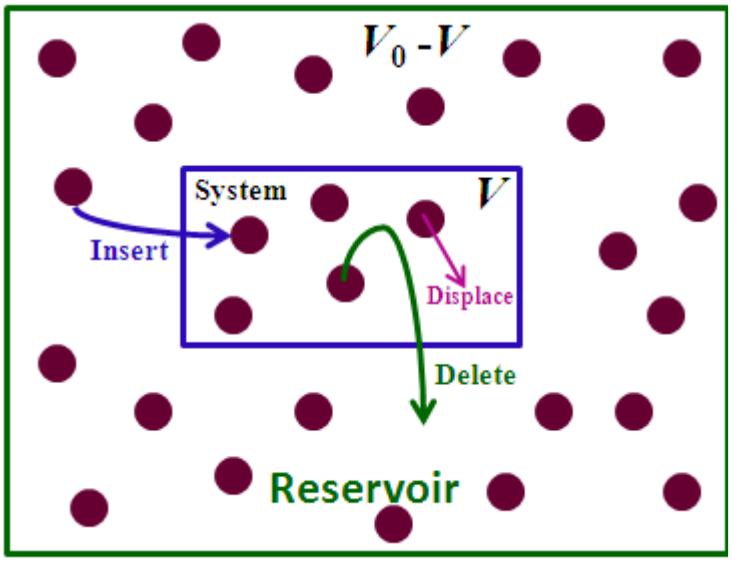

Figure 3.2 A schematic of GCMC basic moves during simulation.

In the current work, we have used GCMC technique to study the phase transition and interfacial property of confined fluid. More particularly, we have used the technique known as Grand canonical transition matrix Monte Carlo (GC-TMMC) along with a multicanonical sampling scheme to discover the configuration space more competently. Further, histogram reweighting technique is employed to situate the coexisting phases. Moreover, for chain molecules united atom approach is used, where we ignore the hydrogen atoms; however, the influence of hydrogen atoms is considered through the parameterisation of potential parameters. Additionally, for chain molecules a configurational- bias technique is incorporated within the GC-TMMC framework.

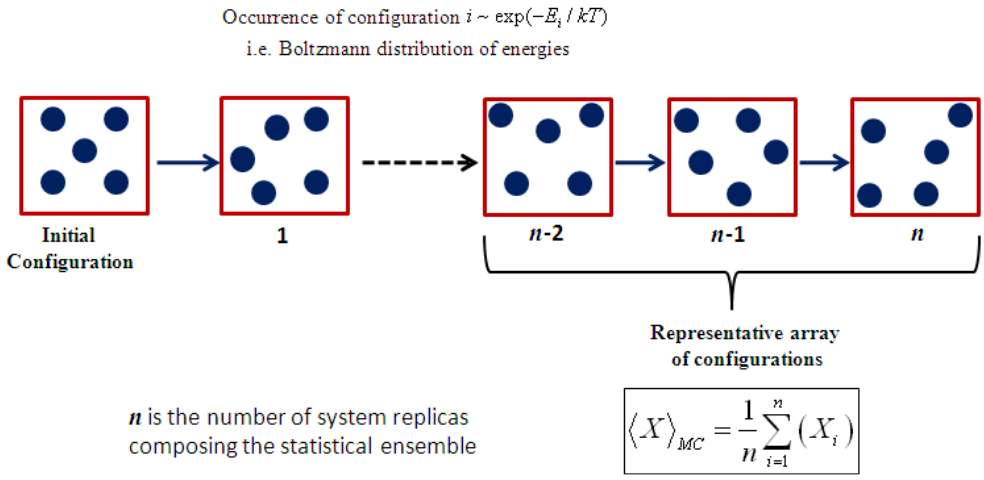

3.2 Simulations Methods

3.2.1 Potential Model

A united-atom approach[58] is used to model the n-alkane molecules. Nonbonded site-site interactions are described with the modified Buckingham exponential intermolecular potential of Errington and Panagiotopoulos[59], for which the pair interaction energy, U, is represented as

$$U(r) = \left\{ \frac{\varepsilon}{1-\frac{6}{\alpha}} \left[\frac{6}{\alpha} \exp\left(\alpha \left[1 - \frac{r}{r_m} \right] \right) - \left(\frac{r_m}{r} \right)^6 \right] \right\} \quad \text{For } r > r_{max}$$

$$= \infty \qquad \text{For } r < r_{max} \qquad (1)$$

Where ε, r_m and α are adjustable parameters. The variable r_m is radial distance at which U(r) reaches a minimum, and the cutoff distance r_{max} represents the smallest radial

distance for which $d[U(r)]/d(r)=0$. The radial distance for which U(r) = 0 is denoted by σ.The parameters U(r) are 129.63K, 3.679 Å, and 16, respectively, for the methyl group (-CH_3), and 73.5K, 4.00 Å, and 22, respectively, for methylene group (-CH_2), and 160.3 K, 3.73 Å, and 15 respectively, for CH_4.

The following combining rules are used to determine the cross parameters:

$$\sigma_{ij}=\frac{1}{2}\left(\sigma_i+\sigma_j\right)$$
$$\varepsilon_{ij}=\left(\varepsilon_i\varepsilon_j\right)^{1/2} \qquad (2)$$
$$\alpha_{ij}=\left(\alpha_i\alpha_j\right)^{1/2}$$

Table 1. Bond lengths of the following compounds.

Compound	**Bond length (Å)**
CH3-CH3	1.839
CH_3-CH_2	1.687
CH_2-CH_2	1.535

Bond-bending angles are generated according to the bending potential.

$$u_{bend}(\theta)=\frac{K_\theta}{2}\left(\theta-\theta_{eq}\right)^2 \qquad (3)$$

Where K_θ =62500 K/rad^2 and θ_{eq} = 114^0. Torsion angles are generated according to the potential.

$$u_{tor(\varphi)}=V_0+\frac{V_1}{2}\left(1+\cos\varphi\right)+\frac{V_2}{2}\left(1-\cos 2\varphi\right)+\frac{V_3}{2}\left(1+\cos 3\varphi\right) \qquad (4)$$

Where V_0 = 0, V_1 = 355.03 K, V_2 = -68.19 K, and V_3 = 791.32 K.

In this work, pore is of slit geometry with smooth and structureless surface. Wall-fluid interaction is described by 9-3 Steele potential.

$$\varphi_{wf(z)} = \frac{2}{3}\pi\rho_w\varepsilon_{wf}\sigma_{wf}{}^3\left\{\frac{2}{15}\left(\frac{\sigma_{wf}}{z}\right)^9 - \left(\frac{\sigma_{wf}}{z}\right)^3\right\} \qquad (5)$$

Where Z is the distance of the fluid particle from the wall and ρ_w, ε_{wf} and σ_{wf} the parameters of the Steele potential[60]. In Eq.(5) $\sigma_{wf} = (\sigma_w + \sigma_{ii})/2$ where σ_w denotes the "diameter" of a wall atom and σ_{ii} refers to the molecular diameter of corresponding CH_2-CH_2 or CH_3-CH_3- interactions.

Table 2. Potential parameters for graphite and mica surfaces.

Potential Parameters	**Graphite**	**Mica**
ρw	0.033 $Å^{-3}$	0.097 $Å^{-3}$
ϵwf	84 K	100 K
σw	3.92 Å	2.22 Å
σwf	3.7995Å	2.9805 Å

3.2.2 Simulation Details

In this work, we have used grand-canonical transition-matrix Monte Carlo (GC-TMMC) simulation technique[7,5,12,13] mostly due to ease of utilizing the parallel processors and efficiency over Monte Carlo techniques[53]. GC-TMMC simulations are conducted with 30 % displacement, 35% insertion and 35% deletion moves. Periodic boundary conditions were implemented in the unconfined directions.

The macroscopic probability is calculated by summing all the microstate states at a constant number of particles. A book keeping scheme of the transition matrix is engaged

to obtain the macroscopic probability. In this format, for each Monte Carlo move ewe record the acceptance probability in a matrix, despite of whether the move is being received or not. Moreover, to make sure a uniform sampling across all densities, we have employed multicanonical sampling scheme[54]. Histogram reweighing method[55] is utilized to obtain the coexistence chemical potential. At specified coexistence chemical potential, we would examine two peaks in the microstate probability distribution as shown in Figure 3.2.2

The minimum and maximum particles numbers are set to make sure the complete sampling of both liquid and vapour phases. The minimum particle number is set to zero and the maximum particle number is set such that the probability of observing maximum particle number at coexistence is less than a particular tolerance[12].

The detailed scheme of this method is described elsewhere[12,56]. GC-TMMC simulation can also yield the interfacial free energy, $F_{L,}$ for a finite system size with box length L, which is determined from the maximum probabilities in the liquid $\prod_{\max}^{l}$ and vapour regions $\prod_{\max}^{v}$, and the minimum probability $\prod_{\min}$ in the interface region (i.e. the region enclosed by the two maxima):

$$\beta F_L = \frac{1}{2}\left(\ln \prod\nolimits_{\max}^{l} + \ln \prod\nolimits_{\max}^{v} \right) - \ln \prod\nolimits_{\min} \qquad (6)$$

Where β denotes the inverse temperature (β =1/*K*T, where K is Boltzmann's factor). This technique does not involve establishing and maintaining an interface, as required in slab-based methods[57]. Figure 1 depicts the interfacial free energy, F_L, in a coexistence probability distribution at different temperatures.

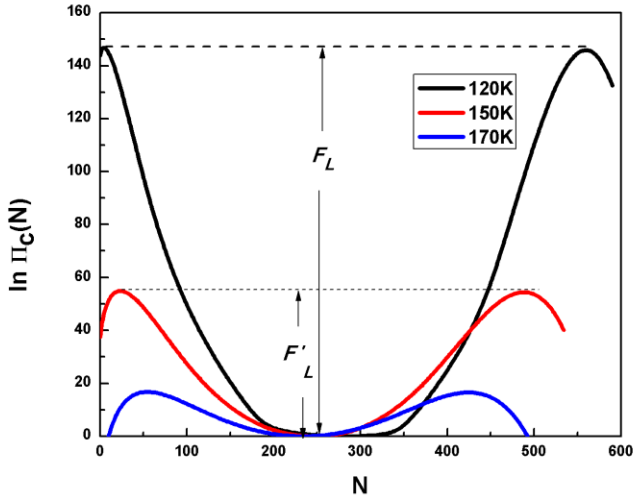

Figure 3.2.2. Schematic of the particle number probability distribution at vapour-liquid phase coexistence condition. The dimensional vapour-liquid interfacial free energy, F_L, is also depicted.

In this work, the interfacial free energy between vapour and liquid phases, F_L, is expected for a given system size and with various temperature in an suitable temperature range using GC-TMMC simulation and histogram reweighting technique. The free energy data, F_L, obtained polynomial fitting with formula;

$$T = A + BFL + CFL^2 \qquad (7)$$

Where, T and F is dimensional Temperature and interfacial free energy, respectively, and A, B and C are fitting parameters to estimate the temperature corresponding to zero F_L. The temperature corresponding to zero F_L is the estimated critical temperature, TC, which is in this case is same as the value of the fitting parameter A.

In this work, we have used a configurational-bias[61,62] grand canonical transition-matrix Monte Carlo (GC-TMMC)[63,64] simulation scheme to explore the configuration space more efficiently. A configurational-bias[61,62] Monte Carlo technique is incorporated within the GC-TMMC framework along with a multicanonical sampling scheme[65]. In this approach, Monte Carlo simulations are conducted in a standard grand-canonical ensemble, where the volume (V), chemical potential, and temperature (T) are held constant and the particle number (N), density and energy (U) fluctuates. During a

simulation, attempted transitions between states of different densities are monitored[66,67]. At usual intervals during a simulation, this information is use to estimate of the density probability distribution, which is consequently used to bias the sampling to low probability densities. Over time, all densities of interest to sampled sufficiently. The result is an efficient self-adaptive method for influential the density probability distribution over a particular range of densities (typically a range that corresponds to the densities of two potentially coexisting phases). Once a probability distribution has been composed at the given value of chemical potential (μ_0), histogram reweighting[68] is used to shift the probability distribution to other value of chemical potential using the following relationship:

$$\ln \prod(N,\mu) = \ln \prod(N,\mu_0) + \beta(\mu - \mu_0)N \qquad (8)$$

To determine the coexistence chemical potential, we apply the above relationship to estimate the chemical potential that produces a coexistence probability distribution.

In this work, we have estimated the vapour-liquid critical parameter by fitting the coexistence densities to the law of the rectilinear diameter and the scaling law for the density.

$$\rho_l + \rho_V = B\left(1 - \frac{T}{T_c}\right)^{\beta} \qquad (9)$$

Where ρ_l, ρ_V, T_c, and β are the liquid-phase density, vapour-phase density, critical temperature, and critical exponent, respectively.

To complete the simulation in an efficient manner, we take advantage of the fact that the TMMC algorithm enables one to fill the overall collection matrix through a sequence of independent simulations, each restricted to a limited range of macrostates.

CHAPTER-4

4. RESULT AND DISCUSSION

In the current work, we have used vapour-liquid interfacial free energy (F_L) of finite size systems to estimate the critical temperature corresponding to zero F_L of bulk and confined alkanes (methane, n-butane, n-octane) .

4.1 Estimation of critical temperature of bulk methane

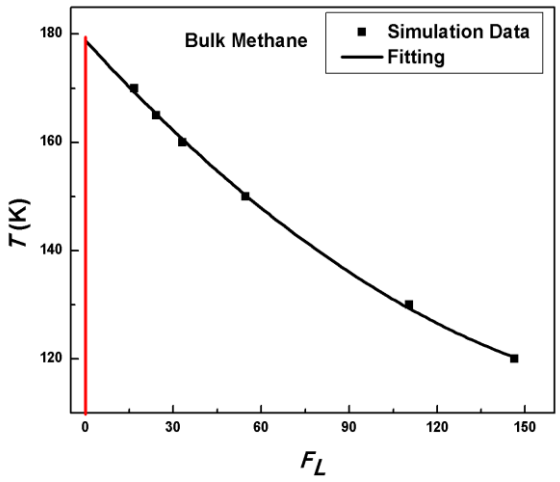

Figure 4.1. Temperature, T, vs. non-dimensional vapour-liquid interfacial free energy F_L = (βF_L) is plotted and fitted with second degree polynomial for bulk.

Figure 4.1 shows interfacial free energy (F_L), at various temperatures for Bulk. The second-degree polynomial fitting for bulk F_L are also shown in Figure 4.1. In this investigation the system volume (V) considered for bulk fluid is 27000 $Å^3$. The temperature is varied from 120 K to 180 K for bulk fluid to estimate the corresponding F_L.

4.2 Estimation of critical temperature of methane confined in graphite slit pore

Figure 4.2(a) and 4.2(b) shows interfacial free energy (F_L), at various temperatures for confined Graphite-methane in slit width, H(Å) = 40, 15, 10, 9, 8, 6, 5.7, and 5.4.The second-degree polynomial fitting for confined Graphite-methane F_L are also shown in Figure 4.2(a) and 4.2(b). In this investigation the system volume (V) considered for H (Å) = 40, 15, 10, 9, 8, 6, 5.7, and 5.4 are 36000 Å^3, 37500 Å^3, 36000 Å^3, 44100 Å^3, 51200 Å^3, 48600 Å^3, 46170 Å^3 and 43740 Å^3, respectively.

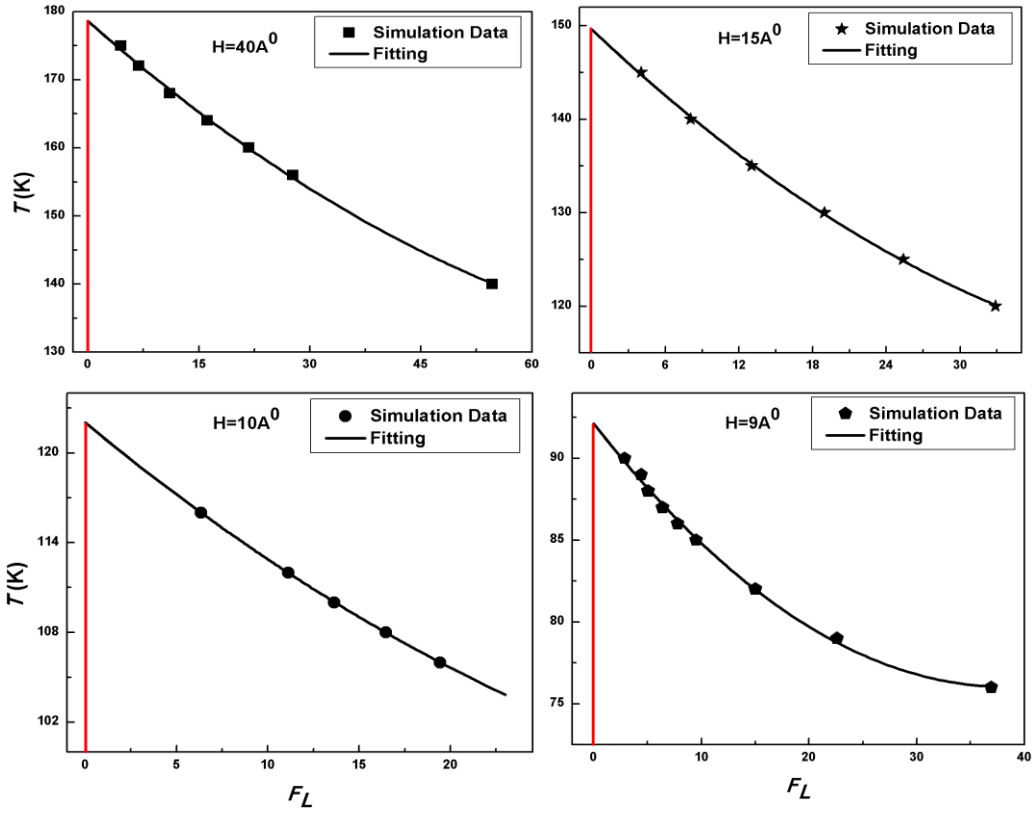

Figure 4.2(a). Temperature, T, vs. non-dimensional vapour-liquid interfacial free energy F_L = (βF_L) is plotted and fitted with second degree polynomial for methane confined in graphite slit pore.

The temperature for H = 40 Å is varied from 140 K to 156 K; for H = 15 Å temperature is varied from 120 K to 145 K; for H = 10 Å temperature is varied from 106 K to 116 K;

for H = 9 Å temperature is varied from 76 K to 90 K; for H = 8 Å temperature is varied from 68 K to 80 K; for H = 6 Å temperature is varied from 68 K to 76 K; for H = 5.7 Å temperature is varied from 68 K to 76 K; for H = 5.4 Å temperature is varied from 68 K to 76 K to estimate the corresponding F_L. The vapour- liquid free energy data, F_L, obtained in various cases are fitted with the second-degree polynomial to get the T corresponding to zero F_L, as depicted in Figure 4.2 (a) and 4.2 (b).

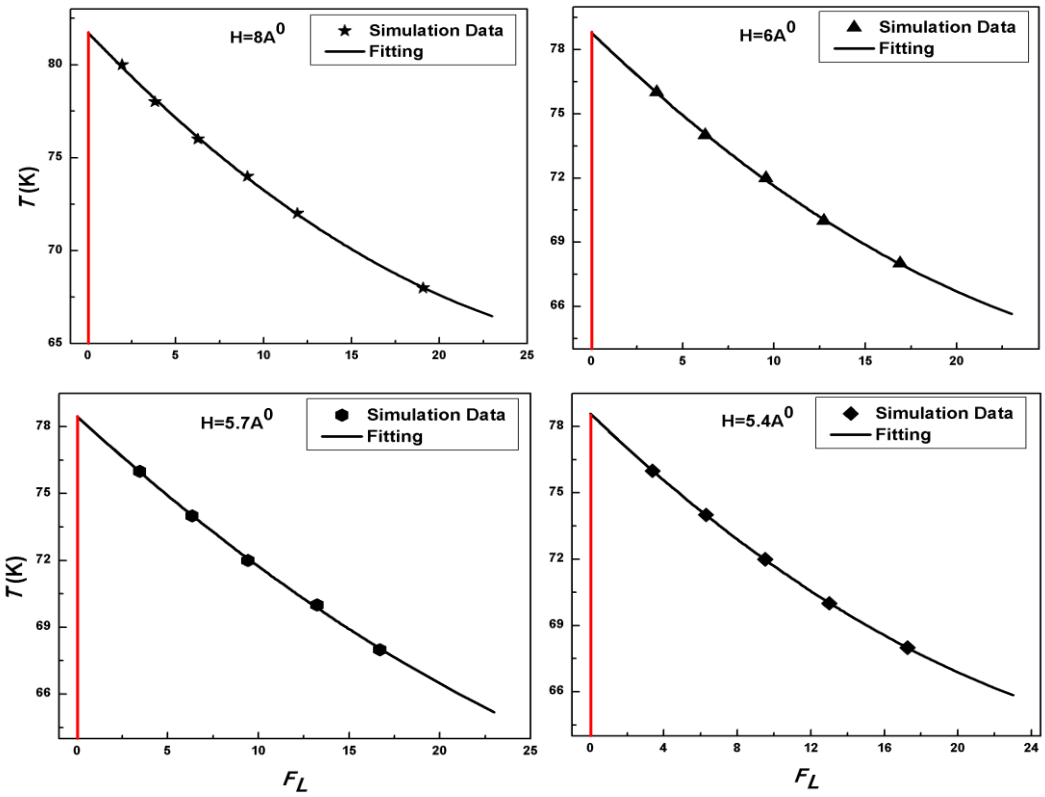

Figure 4.2(b). Temperature, T, vs. non-dimensional vapour-liquid interfacial free energy F_L = (βF_L) is plotted and fitted with second degree polynomial for methane confined in graphite slit pore.

4.3 Estimation of critical temperature of methane confined in mica slit pore

Figure 4.3 (a) and 4.3 (b) shows interfacial free energy (F_L), at various temperatures for confined Mica-methane in slit width, H (Å) = 40, 10, 9, 8.3, 8, 7, 6, 5.4, and 5. The second-degree polynomial fitting for confined Mica-methane F_L are also shown in Figure 4.3 (a) and 4.3 (b) In this investigation the system volume (V) considered for H (Å) = 40, 10, 9, 8.3, 8, 7, 6, 5.4, and 5 are 36000 $Å^3$, 36000 $Å^3$, 44100 $Å^3$, 53120 $Å^3$, 51200 $Å^3$, 44800 $Å^3$, 48600 $Å^3$ and 43740 $Å^3$, and 50000 $Å^3$ respectively.

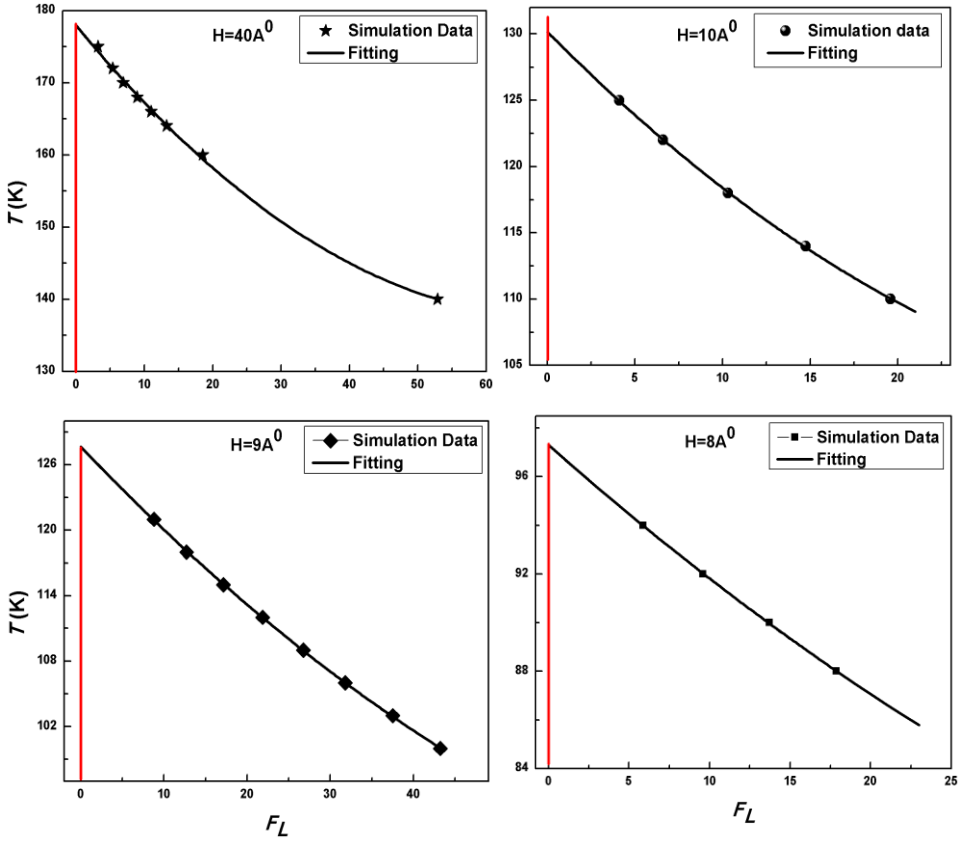

Figure 4.3(a). Temperature, T, vs. non-dimensional vapour-liquid interfacial free energy $F_L = (\beta F_L)$ is plotted and fitted with second degree polynomial for methane confined in mica slit pore.

The temperature for H = 40 Å is varied from 140 K to 175 K ; for H = 10 Å temperature is varied from 110 K to 125 K; for H = 9 Å temperature is varied from 100 K to 121 K; for H= 8.3 Å temperature is varied from 94 K to 108 K; for H = 8 Å temperature is varied from 88 K to 94 K; for H = 7 Å temperature is varied from 70 K to 78 K ; for H = 6 Å temperature is varied from 68 K to 76 K; for H = 5.4 Å temperature is varied from 68 K to 76 K; for H = 5 Å temperature is varied from 68 K to 76 K to estimate the corresponding F_L. The vapour-liquid free energy data, F_L, obtained in various cases are fitted with the second-degree polynomial to get the T corresponding to zero F_L, as depicted in Figure 4.3.1 and 4.3.2.

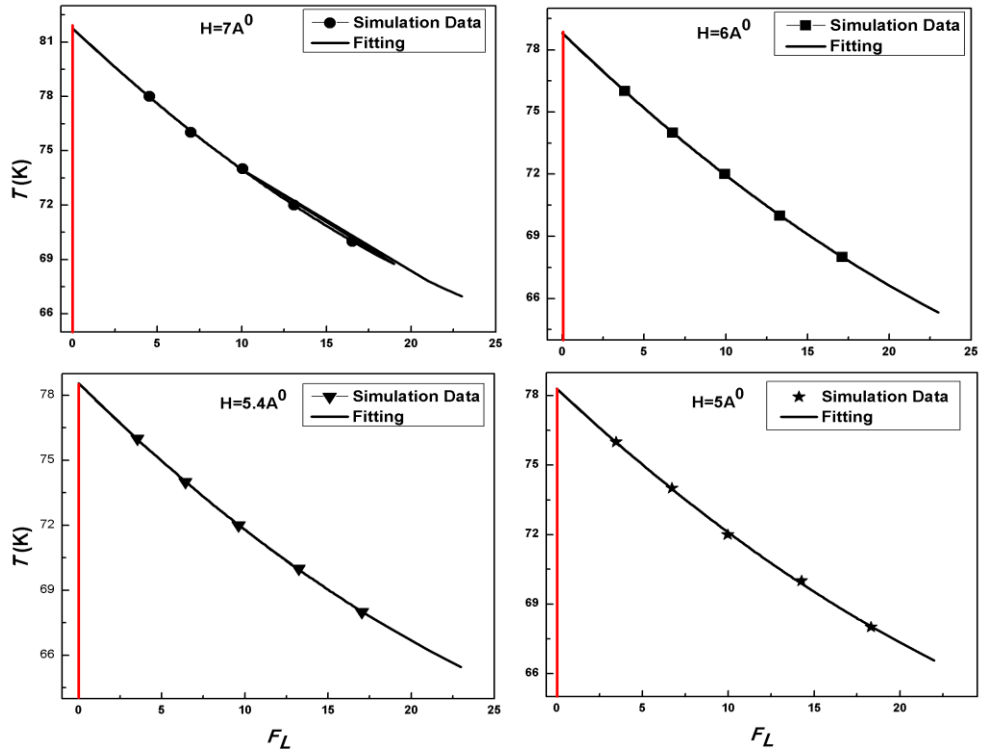

Figure 4.3(b). Temperature, T, vs. non-dimensional vapour-liquid interfacial free energy $F_L = (\beta F_L)$ is plotted and fitted with second degree polynomial for methane confined in mica slit pore.

4.4 Critical temperature of bulk and confined methane and corresponding fitting parameters.

The Temperature (K) corresponding to zero interfacial free energy (F_L) is estimated critical temperature, T_c. The values of fitting parameters A, B and C for the studies cases are reported in Table 1. The estimated critical temperatures, T_c, using this technique are reported in the following Table1.

Table 1. Critical temperature, T_c of bulk and confined methane in Graphite and Mica slit pores of various slit width (H). The system volume, V, considered in each simulation is also included. The corresponding second-degree polynomial fitting parameters A, B and C are also included.

- Polynomial fitting of interfacial free energy, F_L :
- Formula used: $T = A + BF_L + CF_L^2; F_L = 0$ at T = T_c

Slit width H (Å)	System Vol.(V) (Å^3)	A=T_c	B	C
Bulk	27000	178.86532±0.9117	-0.59633±0.03253	0.00134±1.99E-04
Graphite				
40	36000	178.60521±0.51725	-0.96066±0.04718	0.00468±7.67E-04
15	37500	149.61601±0.3976	-1.24386±0.05184	0.01055±0.00138
10	36000	122.00756±0.08497	-1.00594±0.01418	0.00939±5.46E-04
9	44100	92.12544±0.22623	-0.83992±0.03418	0.01097±8.56E-04
8	51200	81.72373±0.18043	-0.9882±0.04194	0.01416±1.93E-03
6	48600	78.79909±0.21103	-0.8289±0.04724	0.01119±2.26E-03
5.7	46170	78.46157±0.26308	-0.74635±0.06016	0.00737±2.92E-03
5.4	43740	78.57246±0.06605	-0.79272±0.01471	-0.79272±0.01471
Mica				
40	36000	177.95494±0.47167	-1.15189±0.05713	0.00822±9.60E-04
10	36000	130.15307±0.23537	-1.33238±0.04666	0.0156±1.94E-03
9	44100	127.63702±0.16963	-0.79568±0.0148	0.00364±2.81E-04
8.3	53120	110.76613±0.1783	-0.60684±0.02194	0.00379±5.31E-04
8	51200	97.31219±0.19645	-0.58608±0.03651	0.00369±0.00152
7	44800	81.76157±0.2545	-0.88319±0.05402	0.01042±2.53E-03
6	48600	78.8119±0.04011	-0.7633±0.00869	0.0077±4.07E-04
5.4	43740	78.56096±0.09312	-0.75883±2.08E-02	0.00824±9.90E-04
5	50000	78.31118±0.24359	-0.695±5.18E-02	0.00732±2.32E-03

4.5 Comparison of the estimated critical temperature of bulk and confined methane using two different methods

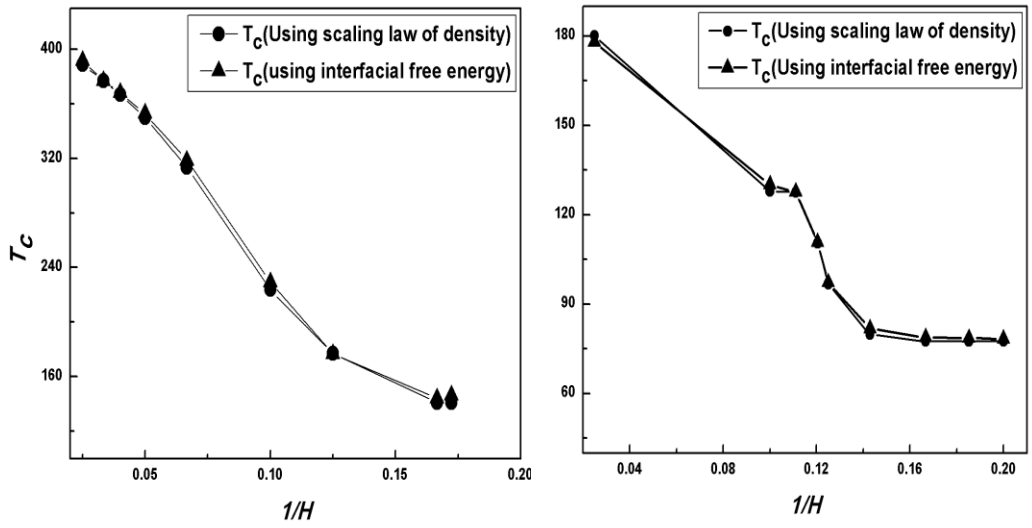

a) Graphite-methane b) Mica-methane

Figure 4.5. Dependence of critical temperature, T_c on the inverse slit width (1/H) is shown for investigated confined methane a) Graphite-methane b) Mica-methane and compared with that obtained using simplified form of scaling law.

The estimated T_c for bulk and confined graphite methane is further compared with the T_c estimated using simplified from scaling law[5] and the comparison is shown in the Table 2 and in Figure 4.5. It can be seen that the T_c estimated using both the techniques follow the same trend for bulk and the confined methane (Graphite-methane and Mica-methane) H (Å) = 40, 15, 10, 9, 8, 6, 5.7, 5.4 b) and H (Å) = 40, 10, 9, 8.3, 8, 7, 6, 5.4, 5 respectively. Moreover, T_c estimated using F_L is differs by 2.8 K, 0.5 K, 1.13K, 1.1 K, 2.3 K, 1.7 K, 1.3 K, 1.3 K, 2.1 K, 2.2 K, 0.1 K, 0.3 K, 0.4 K, 1.8 K, 1.3 K, 1.0 K, and 0.6 K than the T_c estimated using simplified form of scaling law, for the studied bulk and confined methane. This clearly shows insignificant difference in the estimated T_c's using the above two techniques.

Table 2. Comparison of the estimated critical temperature T_c of bulk and confined methane (Graphite-methane and Mica-methane) using two different methods is tabulated.

Slit width (H)	1/H	Scaling Law(T_c) K	Interfacial Free Energy(T_c) K
Bulk	0	188.582	178.86532
Graphite			
40	0.025	181.424	178.60521
15	0.066667	150.152	149.61601
10	0.1	120.87207	122.00756
9	0.111111	91.01624	92.12544
8	0.125	79.4081	81.72373
6	0.166667	77.0453	78.79909
5.7	0.175439	77.122	78.46157
5.4	0.185185	77.23958	78.57246
Mica			
40	0.025	180.119	177.95494
10	0.1	127.953	130.15307
9	0.111111	127.5006	127.63702
8.3	0.120482	110.403	110.76613
8	0.125	96.85328	97.31219
7	0.142857	79.8622	81.76157
6	0.166667	77.46667	78.8119
5.4	0.185185	77.5073	78.56096
5	0.2	77.6433	78.31118

In Figure 4.5, comparison of the critical temperature, T_c estimated by the two methods, is shown with respect to inverse of the slit width, h. In this Figure 4.5, T_c estimation is compared using the simplified form of scaling law of density[5] and the T_c estimated corresponding to zero interfacial free energy, F_L. In the Figure 4.5, T_c of bulk system is also included, which is the case corresponding to 1/H = 0. Moreover, Figure 4.5 shows interesting monotonic decreasing behaviour of T_c with respect to inverse H, irrespective of techniques used to estimate the T_c. Further, with decrease in the slit width, H, the critical temperature T_c decreases monotonically until H = 5.7 Å for confined graphite-methane and for confined Mica-methane H = 5.4 Å; however, for confined graphite-methane $5.7 < H \leq 5.4$ and for confined mica-methane $5.4 < H \leq 5$, T_c becomes

approximately indifferent with change in H. This behaviour primarily indicates significant differences in structural properties of vapour and liquid like phases in various regimes of slit width, as described in the earlier work. These regimes have different slopes, which indicate that the rate of change in T_c is not constant across the studied slit width range. Moreover, simplified form of scaling law[5] indicates that the difference in the coexistence vapour and liquid densities ($\rho l - \rho v$) plays major role in the estimated T_c. The coexistence vapour and liquid densities are the average outcomes of the local structural behaviour of the coexisting phases under confinement. This in turn indicates that the structural changes in fluid phases with degree of confinement play a significant role in their respective average coexistence densities and, hence, on the critical temperature, T_c, as depicted in the earlier work. Interestingly, it is observed that T_c remains indifferent for $H < 5.7$ for confined graphite-methane and $H < 5.4$ for confined mica-methane. On the major reason of this beaviour of T_c is that the maximum possible layer in local structural behaviour is limited to one for $H < 5.7$ for confined graphite-methane and $H < 5.4$ for confined mica-methane. Therefore, the difference in coexistence densities, ($\rho l - \rho v$) becomes approximately indifferent in the extremely small pores and so does the T_c, which eventually approaches to the two- value at H = 5.4 Å for confined graphite-methane and H = 5 Å for confined mica-methane. Moreover, the maximum difference in tc estimated corresponding to the zero F_L and that estimated using the simplified form of the scaling law[5] is less than 1% for the bulk and for confined graphite-methane with $40 \leq H \leq 10$; for confined mica-methane $40 \leq H \leq 9$. Whereas, for the studies with $10 \leq H \leq 5.4$ for confined graphite-methane, $9 \leq H \leq 5$ for confined mica-methane , the maximum differences in the estimation Tc using two techniques is less than 3%.

4.6 Estimation of critical temperature of bulk butane

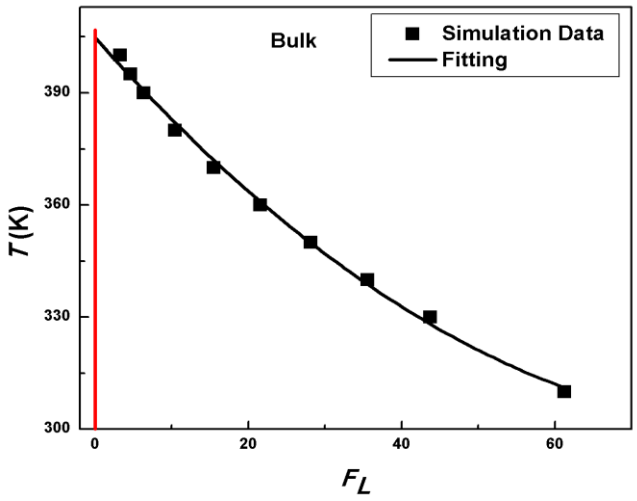

Figure 4.6. Temperature, T, vs. non-dimensional vapour-liquid interfacial free energy F_L = (βF_L) is plotted and fitted with second degree polynomial for bulk.

Figure 4.6 shows interfacial free energy (F_L), at various temperatures for Bulk. The second-degree polynomial fitting for bulk F_L is also shown in Figure 4.6. In this investigation the system volume (V) considered for bulk fluid is 27000 (Å^3). The temperature is varied from 310 K to 400 K for bulk fluid to estimate the corresponding F_L.

4.7 Estimation of critical temperature of butane confined in graphite slit pore

Figure 4.7 (a) and 4.7 (b) shows interfacial free energy (F_L), at various temperatures for confined Graphite-butane in slit width, H(Å) = 40, 30, 25, 20, 15, 10, 8, 6, and 5.8.The second-degree polynomial fitting for confined Graphite-butane F_L are also shown in Figure 4.7 (a) and 4.7 (b). In this investigation the system volume (V) considered for H

(Å) = 40, 30, 25, 20, 15, 10, 8, 6, and 5.8 are 100,000 Å^3, 60,750 Å^3, 50,625 Å^3, 50,000 Å^3, 54,000 Å^3, 64,000 Å^3, 64,800 Å^3, 48,600 Å^3 and 58,000 Å^3 respectively.

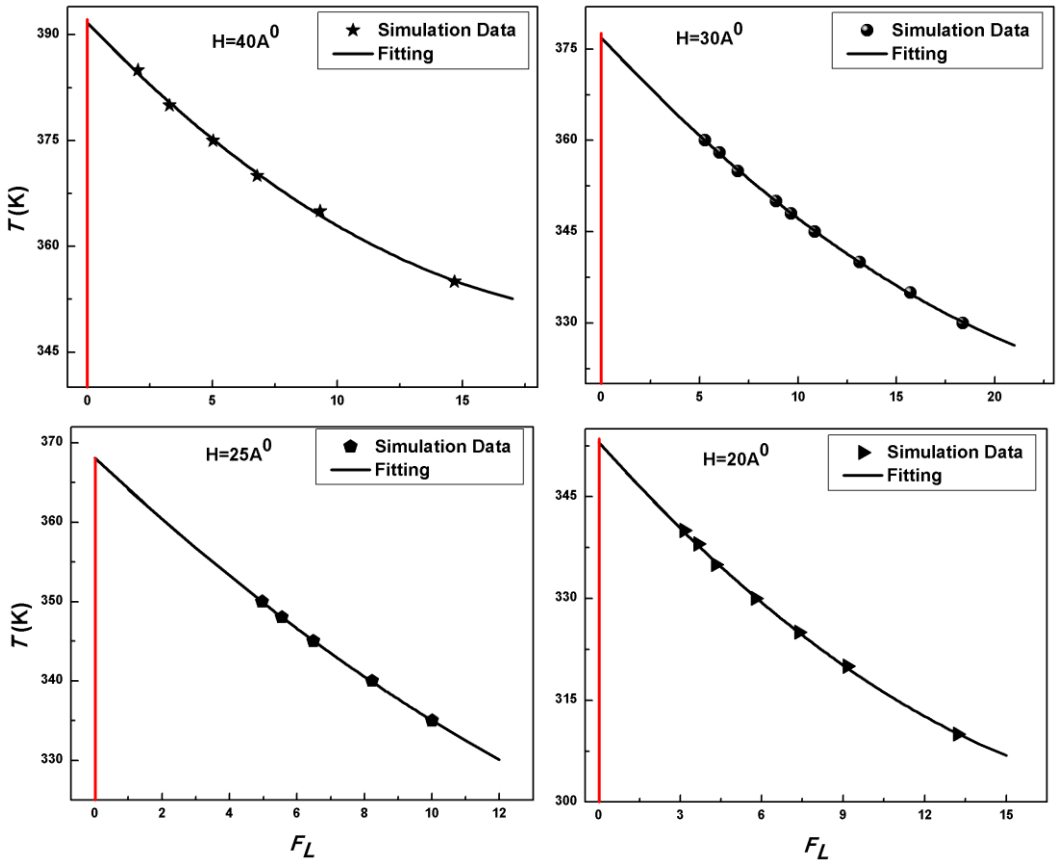

Figure 4.7(a). Temperature, T, vs. non-dimensional vapour-liquid interfacial free energy F_L = (βF_L) is plotted and fitted with second degree polynomial for butane confined in graphite slit pore.

The temperature, for H = 40 Å is varied from 355 K to 385 K; for H = 30 Å, temperature is varied from 330 K to 360 K; for H = 25 Å temperature is varied from 335 K to 350 K; for H = 20 Å temperature is varied from 310 K to 340 K; for H = 15 Å temperature is varied from 290 K to 312 K; for H = 10 Å, temperature is varied from 205 K to 225 K; for H = 8 Å, temperature is varied from 156 K to 166 K; for H = 6 Å temperature is varied from 132 K to 139 K; for H = 5.8 Å temperature is varied from 133

K to 140 K to estimate the corresponding F_L. The vapour- liquid free energy data, F_L, obtained in various cases are fitted with the second-degree polynomial to get the T corresponding to zero F_L, as depicted in Figure 4.7 (a) and 4.7 (b).

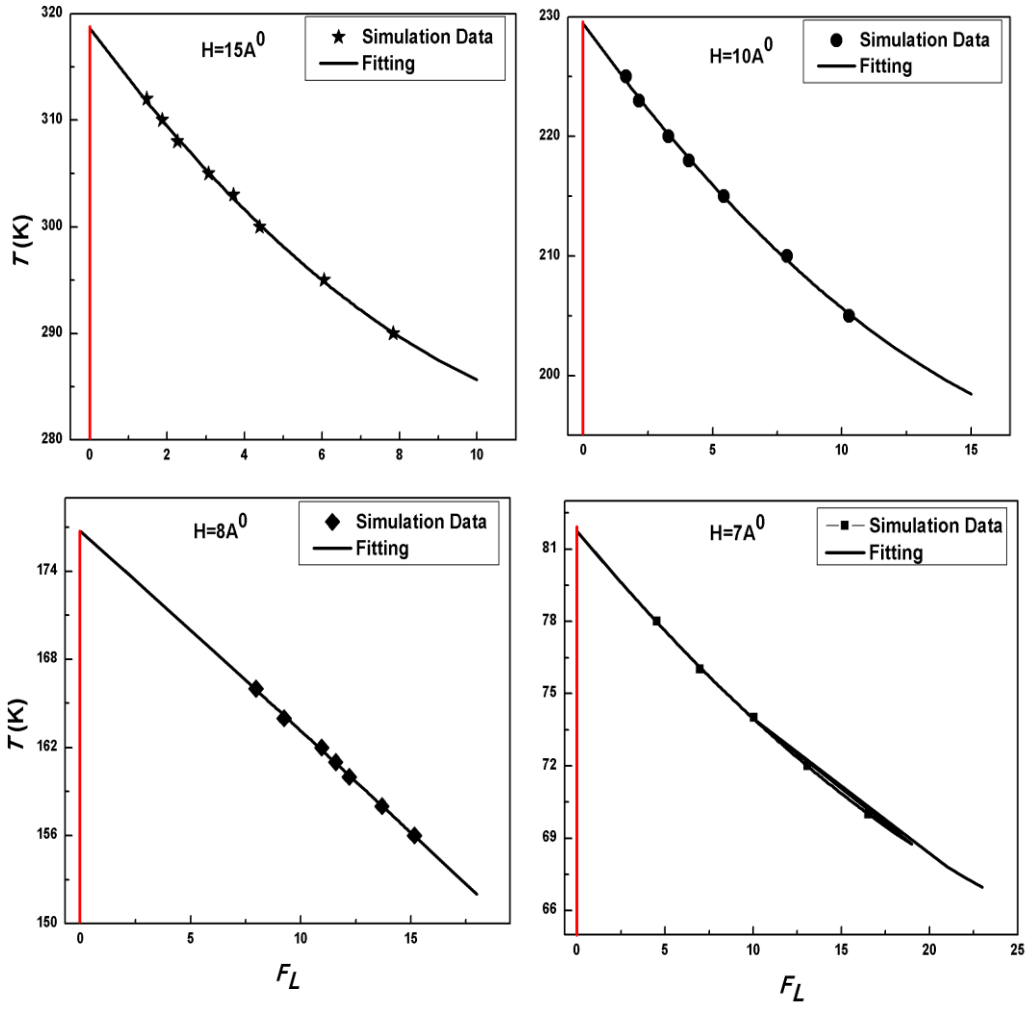

Figure 4.7(b). Temperature, T, vs. non-dimensional vapour-liquid interfacial free energy $F_L = (\beta F_L)$ is plotted and fitted with second degree polynomial for butane confined in graphite slit pore.

4.8 Estimation of critical temperature of butane confined in mica slit pore

Figure 4.8 (a), 4.8 (b) and 4.8 (c) shows interfacial free energy (F_L), at various temperatures for confined mica-butane in slit width, H (Å) = 40, 30, 25, 20, 15, 10, 8, 6, 5.7, and 5.5.The second-degree polynomial fitting for confined mica-butane F_L are also shown in Figure 4.8 (a), 4.8 (b) and 4.8 (c). In this investigation the system volume (V) considered for H (Å) = 40, 30, 25, 20, 15, 10, 8, 6, 5.7, and 5.5 are 100,000 Å^3, 60,750 Å^3, 50,625 Å^3, 50,000 Å^3, 54,000 Å^3, 64,000 Å^3, 64,800 Å^3, 72,600 Å^3, 68,970 Å^3 and 65,340 Å^3 respectively.

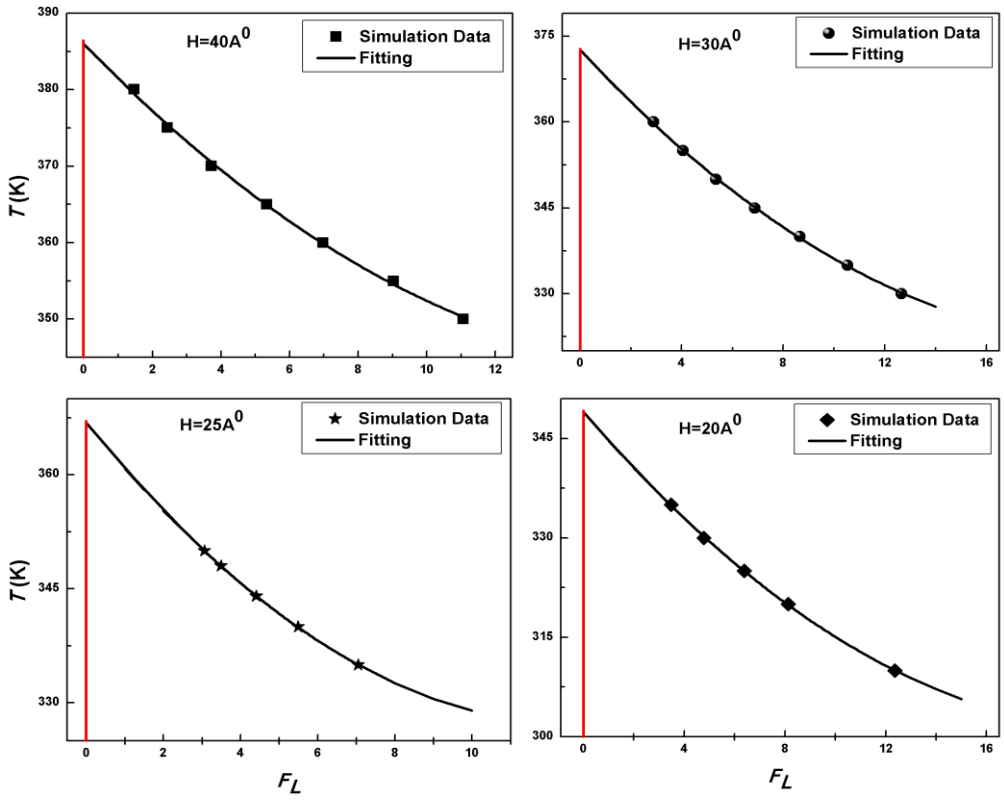

Figure 4.8(a). Temperature, T, vs. non-dimensional vapour-liquid interfacial free energy F_L = (βF_L) is plotted and fitted with second degree polynomial for butane confined in mica slit pore.

The temperature for H = 40 Å is varied from 350 K to 380 K; for H= 30 Å temperature is varied from 330 K to 360 K; for H = 25 Å temperature is varied from 335 K to 350 K; for H= 20 Å temperature is varied from 310 K to 335 K; for H= 15 Å temperature is varied from 295 K to 316 K; for H= 10 Å temperature is varied from 245 K to 265 K; for H= 8 Å temperature is varied from 204 K to 214 K; for H= 6 Å temperature is varied from 140 K to 152 K; for H= 5.7 Å temperature is varied from 138 K to 143 K; for H = 5.5 Å temperature is varied from 138 K to 143 K to estimate the corresponding F_L.

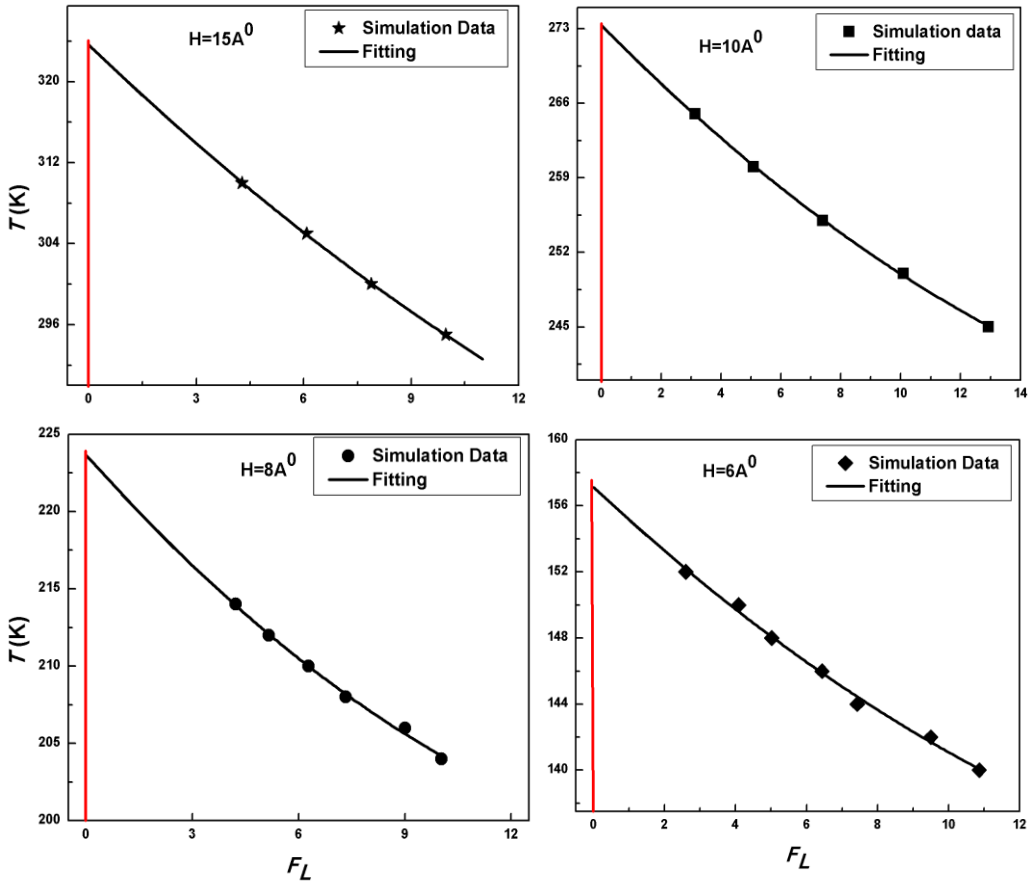

Figure 4.8(b). Temperature, T, vs. non-dimensional vapour-liquid interfacial free energy F_L = (βF_L) is plotted and fitted with second degree polynomial for butane confined in mica slit pore.

The vapour- liquid free energy data, F_L, obtained in various cases are fitted with the second-degree polynomial to get the T corresponding to zero F_L, as depicted in Figure 4.8 (a), 4.8 (b) and 4.8 (c).

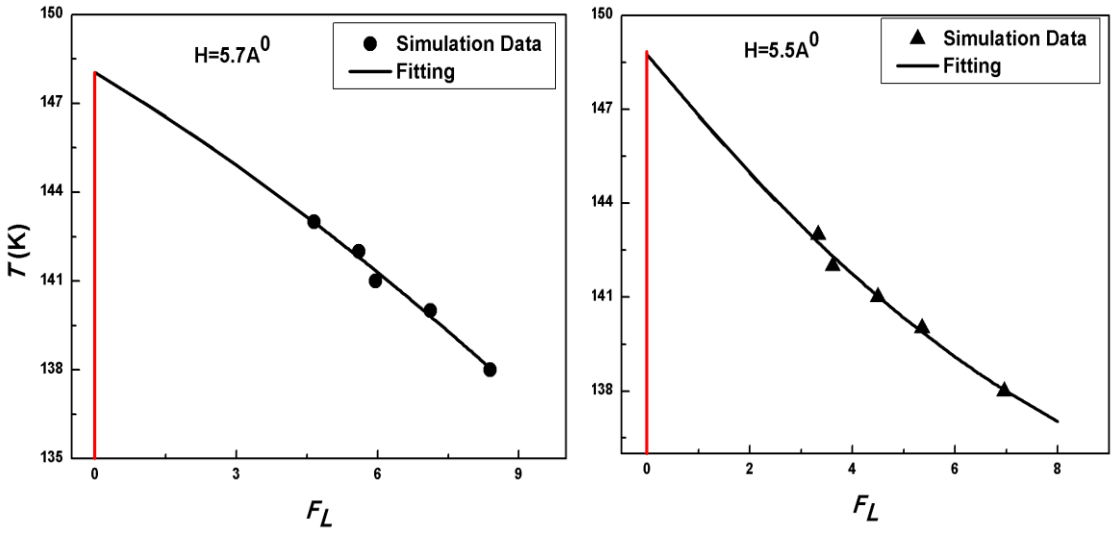

Figure 4.8(c). Temperature, T, vs. non-dimensional vapour-liquid interfacial free energy F_L = (βF_L) is plotted and fitted with second degree polynomial for butane confined in mica slit pore.

4.9 Critical temperature of bulk and confined butane and corresponding fitting parameters

The T(K) corresponding to zero F_L is estimated critical temperature, T_c. The values of fitting parameters A, B and C for the studies cases are reported in Table 3. The estimated critical temperatures, T_c, using this technique are reported in the following table.

Table 3. Critical temperature, T_c of bulk and confined n-butane a) Graphite-butane b) Mica-butane for various slit width, H is tabulated. The system volume, V, considered in

each simulation is also included. The corresponding second-degree polynomial fitting parameter A, B and C are also included.

- Polynomial fitting of interfacial free energy, F_L :
- Formula used: $T = A + BF_L + CF_L^2; F_L = 0$ at T = T_c

Slit width (H)	System Vol. (V) (Å^3)	A = T_c	B	C
Bulk	27000	404.75796±1.33269	-2.30883±2.30883	0.01275±0.00183
Graphite				
40	100,000	391.65691±0.84574	-3.69622±0.11406	0.08233±0.01431
30	60,750	376.90459±0.42413	-3.48162±0.0806	0.051±0.00342
25	50,625	368.06957±1.09944	-3.98613±0.30956	0.06835±0.02058
20	50,000	352.99859±0.59008	-4.50551±0.17145	0.0952±0.01048
15	54,000	318.62604±0.46907	-4.89364±0.24224	0.15933±0.02593
10	64,000	229.38163±0.49871	-2.99593±0.20706	0.06228±0.0172
8	64,800	176.71158±1.31338	-1.33562±0.23301	-0.0021±0.01005
6	48,600	150.10978±0.94402	-3.74691±0.36758	0.20614±0.03397
5.8	58,000	146.33323±0.13421	-2.25727±0.0522	0.07596±0.00459
Mica				
40	100,000	385.95578±0.74941	-4.61598±0.28932	0.126±0.0228
30	60,750	372.55606±0.60651	-4.75297±0.17751	0.11101±0.0113
25	50,625	366.80081±0.48434	-6.24566±0.20532	0.24638±0.02019
20	50,000	348.94453±0.69049	-4.39879±0.19448	0.10121±0.01192
15	54,000	323.6229±0.95341	-3.40306±0.28443	0.05314±0.01977
10	64,000	273.30763±0.52799	-2.8471±0.14939	0.05143±0.00914
8	64,800	223.65386±1.66615	-2.56867±0.49473	0.06278±0.03434
6	72,600	157.10616±0.86843	-1.99767±0.28291	0.03966±0.02048
5.7	68,970	148.04888±4.05172	-0.96293±1.27007	-0.02718±0.09633
5.4	65,340	148.73864±2.34847	-2.03438±0.96688	0.07131±0.09356

4.10 Comparison of the estimated critical temperature of bulk and confined butane using two different methods

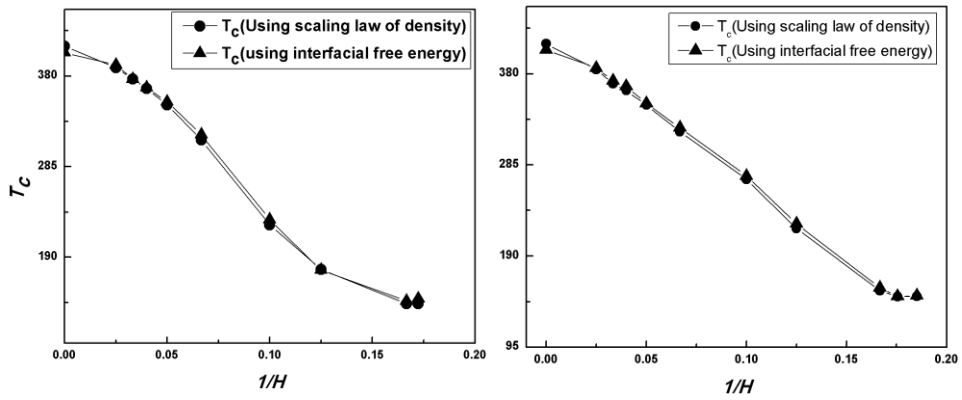

a) Graphite-butane b) Mica-butane

Figure 4.10. Dependence of critical temperature, T_c on the inverse slit width (1/H) is shown for investigated Confined n-butane a) Graphite-butane b) Mica-butane and compared with that obtained using simplified form of scaling law.

The estimated T_c for bulk and confined n-butanae is further compared with the T_c estimated using simplified from scaling law[5] and the comparison is shown in the Table 4 and in Figure 4.10. It can be seen that the T_c estimated using both the techniques follow the same trend for bulk and the confined n-butane (Graphite-butane and Mica-butane) H (Å) = 40, 30, 25, 20, 15, 10, 8, 6, 5.8 and H (Å) = 40, 30, 25, 20, 15, 10, 8, 6, 5.7, 5.4 respectively. Moreover, Tc estimated using F_L is lower by, 6.5 K, 2.6 K, 0.004 K, 1.3 K, 2.9 K, 5.3 K, 5.4 K, 0.4 K, 3.1 K, 5.1 K, 1.6 K, 2.7 K, 4.4 K, 1.6 K, 3.8 K, 3.3 K, 4.9 K, 3.2 K, 0.3 K, and 0.8 K than the T_c estimated using simplified form of scaling law[5], for the studied bulk and confined n-butane. This clearly shows insignificant difference in the estimated Tc's using the above two techniques.

Table 4. Comparison of the estimated critical temperature, T_c of bulk and confined n butane (Graphite-butane and Mica-butane) using two different methods is tabulated.

Slit Width	1/H	Scaling Law (T_c) K	Interfacial Free Energy (T_c) K
Bulk	0	411.278	404.75796
Graphite			
40	0.025	388.98	391.65691
30	0.033333333	376.9	376.90459
25	0.04	366.76	368.06957
20	0.05	350.006	352.99859
15	0.066666667	313.29	318.62604
10	0.1	223.94	229.38163
8	0.125	177.17	176.71158
6	0.166666667	141.19	144.32102
5.8	0.172413793	141.2	146.33323
Mica			
40	0.025	384.35	385.95578
30	0.033333333	369.76	372.55606
25	0.04	362.4	366.80081
20	0.05	347.31	348.94453
15	0.066666667	319.7515	323.6229
10	0.1	269.981	273.30763
8	0.125	218.75	223.65386
6	0.166666667	153.844	157.10616
5.7	0.175438596	147.732	148.04888
5.4	0.185185185	147.87	148.73864

In Figure 4.10, comparison of the critical temperature, T_c estimated by the two methods, is shown with respect to inverse of the slit width, h. In this Figure 4.10, T_c estimation is compared using the simplified form of scaling law of density[5] and the T_c estimated corresponding to zero interfacial free energy, F_L. In the Figure 4.10, T_c of bulk system is also included, which is the case corresponding to 1/H = 0. Moreover, Figure 4.10 shows interesting monotonic decreasing behaviour of T_c with respect to inverse H, irrespective of techniques used to estimate the T_c. Further, with decrease in the slit width, H, the critical temperature T_c decreases monotonically until H = 6 Å for confined graphite-butane and for confined Mica-butane H = 5.7 Å however, for confined graphite-butane $6 < H \leq 5.8$ and for confined mica-butane $5.7 < H \leq 5.4$, T_c becomes approximately indifferent with change in H. This behaviour primarily indicates significant differences in

structural properties of vapour and liquid like phases in various regimes of slit width, as described in the earlier work. These regimes have different slopes, which indicate that the rate of change in T_c is not constant across the studied slit width range. Moreover, simplified form of scaling law[5] indicates that the difference in the coexistence vapour and liquid densities ($\rho l - \rho v$) plays major role in the estimated T_c. The coexistence vapour and liquid densities are the average outcomes of the local structural behaviour of the coexisting phases under confinement. This in turn indicates that the structural changes in fluid phases with degree of confinement play a significant role in their respective average coexistence densities and, hence, on the critical temperature, T_c, as depicted in the earlier work. Interestingly, it is observed that T_c remains indifferent for $H < 6$ for confined graphite-butane and $H < 5.7$ for confined mica-butane. On the major reason of this beaviour of T_c is that the maximum possible layer in local structural behaviour is limited to one for $H < 6$ for confined graphite-butane and $H < 5.7$ for confined mica-butane. Therefore, the difference in coexistence densities, ($\rho l - \rho v$) becomes approximately indifferent in the extremely small pores and so does the T_c, which eventually approaches to the two- value at $H = 5.8$ Å for confined graphite-butane and $H = 5.4$ Å for confined mica-butane. Moreover, the maximum difference in tc estimated corresponding to the zero F_L and that estimated using the simplified form of the scaling law[5] is less than 1% for the bulk and for confined graphite-butane with $40 \leq H \leq 25$; for confined mica-butane $40 \leq H \leq 25$. Whereas, for the studies with $25 \leq H \leq 5.8$ for confined graphite-butane, $9 \leq H \leq 5.4$ for confined mica-butane, the maximum differences in the estimation Tc using two techniques is less than 3%.

4.11 Estimation of critical temperature of bulk octane

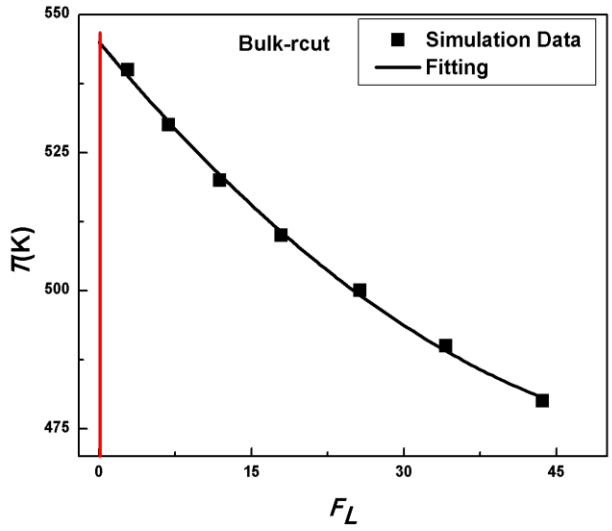

Figure 4.11. Temperature, T, vs. non-dimensional vapour-liquid interfacial free energy $F_L = (\beta F_L)$ is plotted and fitted with second degree polynomial for bulk.

Figure 4.11 shows interfacial free energy (F_L), at various temperatures for Bulk. The second-degree polynomial fitting for bulk F_L Is also shown in Figure 4.11. In this investigation the system volume (V) considered for bulk fluid is 27000 Å^3. The temperature is varied from 480 K to 540 K for bulk fluid to estimate the corresponding F_L.

4.12 Estimation of critical temperature of octane confined in graphite slit pore

Figure 4.12 (a), 4.12 (b) and 4.12 (c) shows interfacial free energy (F_L), at various temperatures for confined Graphite-octane in slit width, H(Å) = 50, 40, 30, 20, 15, 12, 10, 9, 8, 7.The second-degree polynomial fitting for confined Graphite-octane F_L are also shown in Figure 4.12 (a), 4.12(b) and 4.12 (C). In this investigation the system volume (V) considered for H (Å) = 50, 40, 30, 20, 15, 12, 10, 9, 8, 7 are 216000 Å^3 245000 Å^3, 196000 Å^3, 147000 Å^3, 128000 Å^3, 121500 Å^3, 172800 Å^3, 81000 Å^3, 129600 Å^3 and 115200 Å^3, 100800 Å^3 respectively.

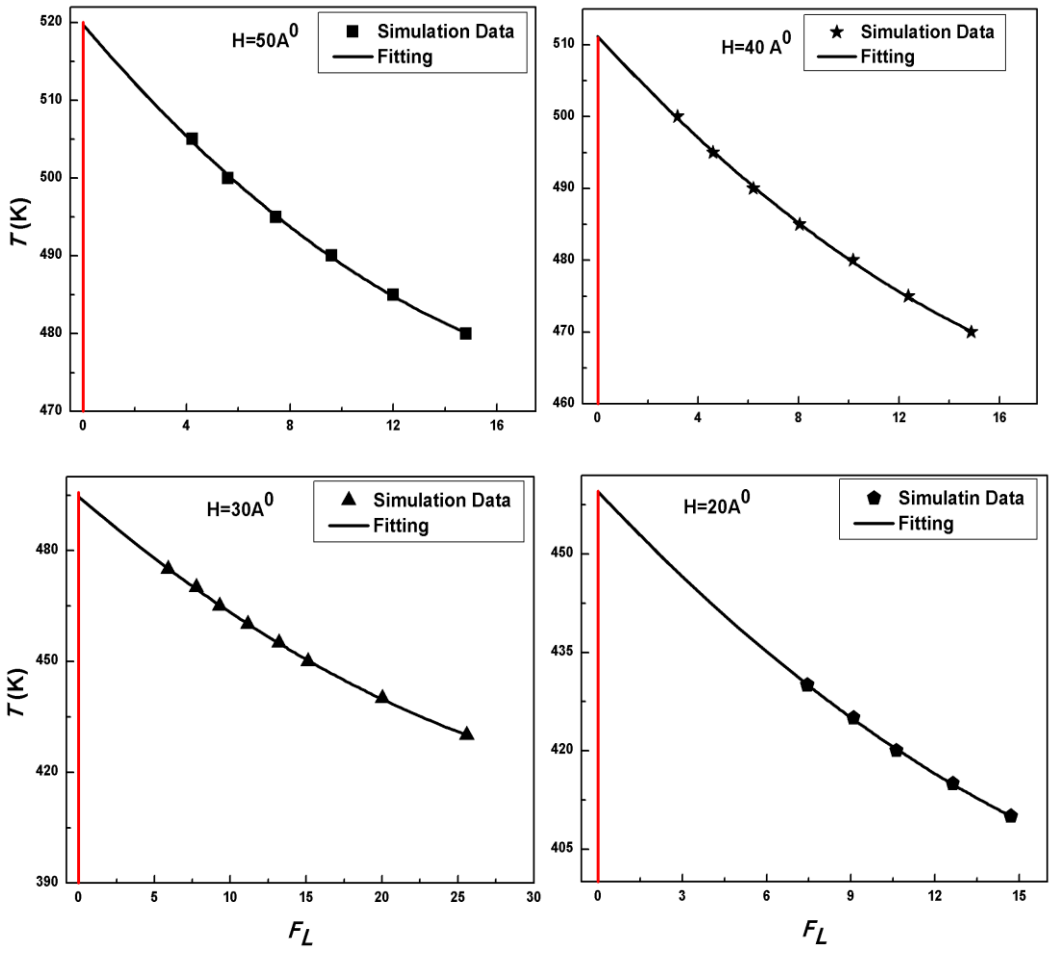

Figure 4.12(a). Temperature, T, vs. non-dimensional vapour-liquid interfacial free energy $F_L = (\beta F_L)$ is plotted and fitted with second degree polynomial for octane confined in mica slit pore.

The temperature for H = 50 Å is varied from 480 K to 505 K; for H= 40 Å temperature is varied from 470 K to 500 K; for H= 30 Å temperature is varied from 430 K to 475 K; for H= 20 Å temperature is varied from 410 K to 430 K; for H= 15 Å temperature is varied from 370 K to 395 K; for H= 12 Å temperature is varied from 326 K to 346 K; for H= 10 Å temperature is varied from 246 K to 256 K; for H= 9 Å temperature is varied from 228 K to 242 K; for H= 8 Å temperature is varied from 212 K to 224 K; for H= 7 Å temperature is varied from 184 K to 190 K to estimate the corresponding F_L.

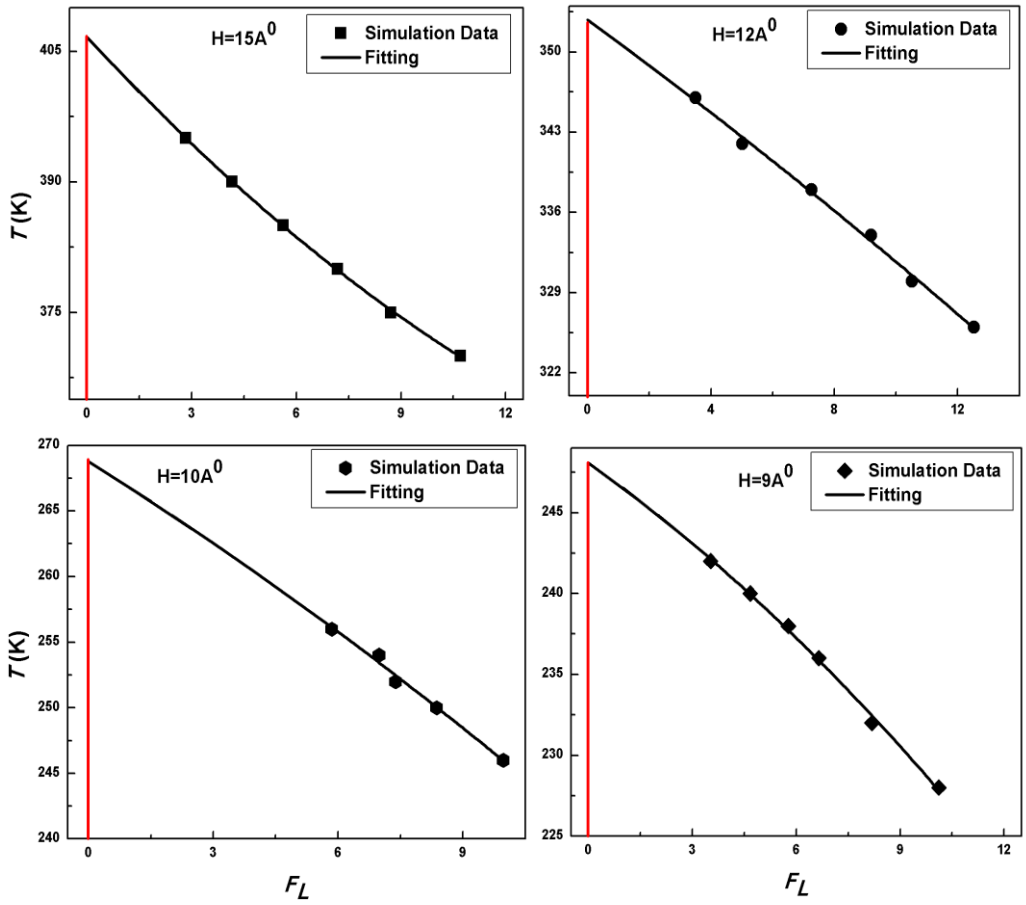

Figure 4.12(b). Temperature, T, vs. non-dimensional vapour-liquid interfacial free energy $F_L = (\beta F_L)$ is plotted and fitted with second degree polynomial for octane confined in mica slit pore

The vapour- liquid free energy data, F_L, obtained in various cases are fitted with the second-degree polynomial to get the T corresponding to zero F_L, as depicted in Figure 4.12 (a), 4.12 (b) and 4.12 (c).

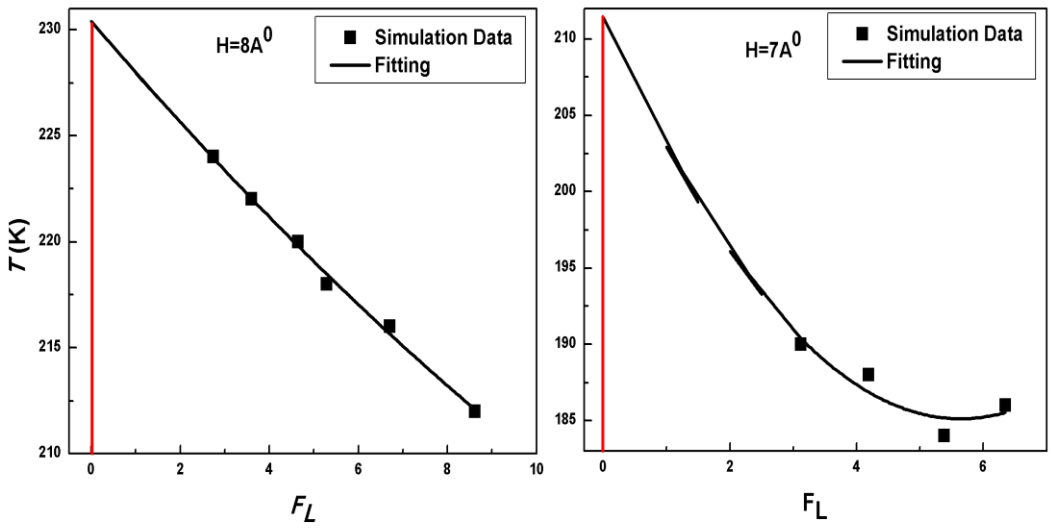

Figure 4.12(c). Temperature, T, vs. non-dimensional vapour-liquid interfacial free energy $F_L = (\beta F_L)$ is plotted and fitted with second degree polynomial for octane confined in mica slit pore.

4.13 Estimation of critical temperature of octane confined in mica slit pore

Figure 4.13 (a) and 4.13 (b) shows interfacial free energy (F_L), at various temperatures confined Mica-octane in slit width, H(Å) = 50, 40, 30, 20, 15, 12, 10, 8, and 7. The second-degree polynomial fitting for confined Mica octane F_L are also shown in Figure 4.13 (a) and 4.13 (b) In this investigation the system volume (V) considered for H (Å) =50, 40, 30, 20, 15, 12, 10, 8, 6.7 and 6.5 are 216000 Å^3, 245000 Å^3, 196000 Å^3, 147000 Å^3, 128000 Å^3, 121500 Å^3, 81000 Å^3, 115200 Å^3, 96480 Å^3 and 93600 Å^3 respectively.

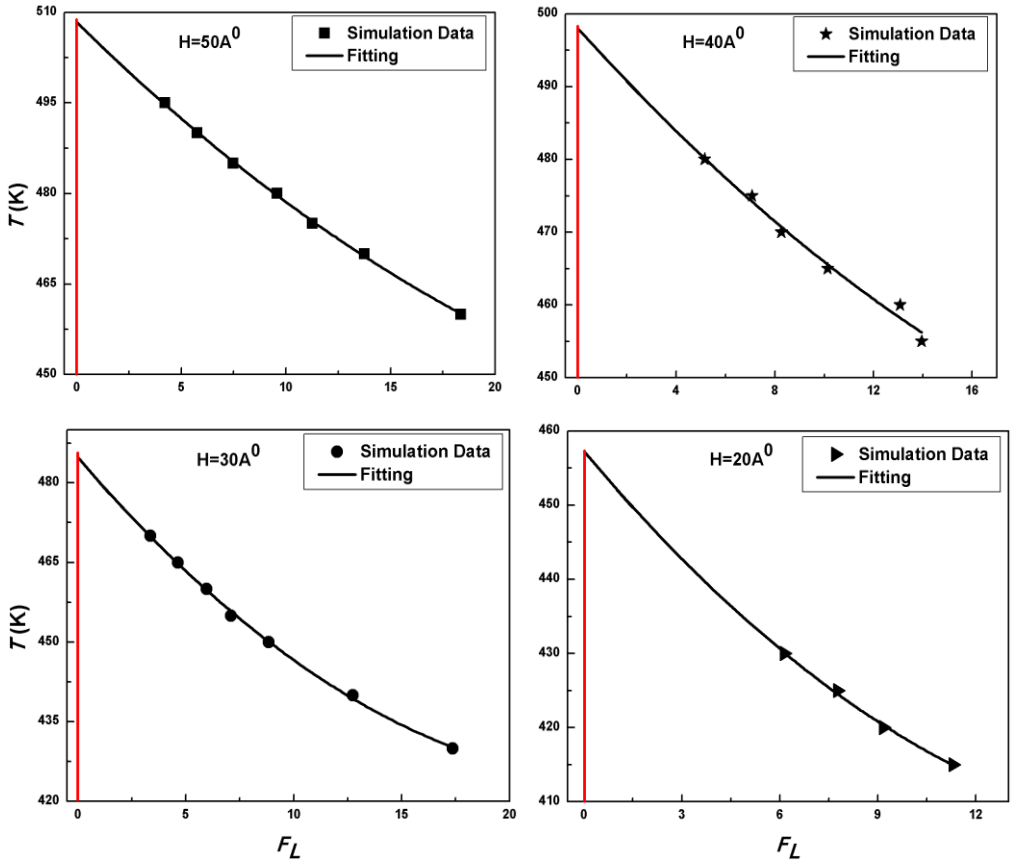

Figure 4.13(a). Temperature, T, vs. non-dimensional vapour-liquid interfacial free energy $F_L = (\beta F_L)$ is plotted and fitted with second degree polynomial for octane confined in mica slit pore.

The temperature for H = 50 Å temperature is varied from 460 K to 495 K; for H= 40 Å temperature is varied from 455 K to 480 K; for H= 30 Å temperature is varied from 430 K to 470 K; for H= 20 Å temperature is varied from 415 K to 430 K; for H= 15 Å temperature is varied from 375 K to 405 K; for H= 10 Å temperature is varied from 302 K to 333 K; for H= 8 Å temperature is varied from 242 K to 255 K; for H= 7 Å temperature is varied from 228 K to 234 K; for H= 6.7 Å temperature is varied from 218 K to 226 K; for H= 6.5 Å temperature is varied from 212 K to 222 K to estimate the corresponding F_L.

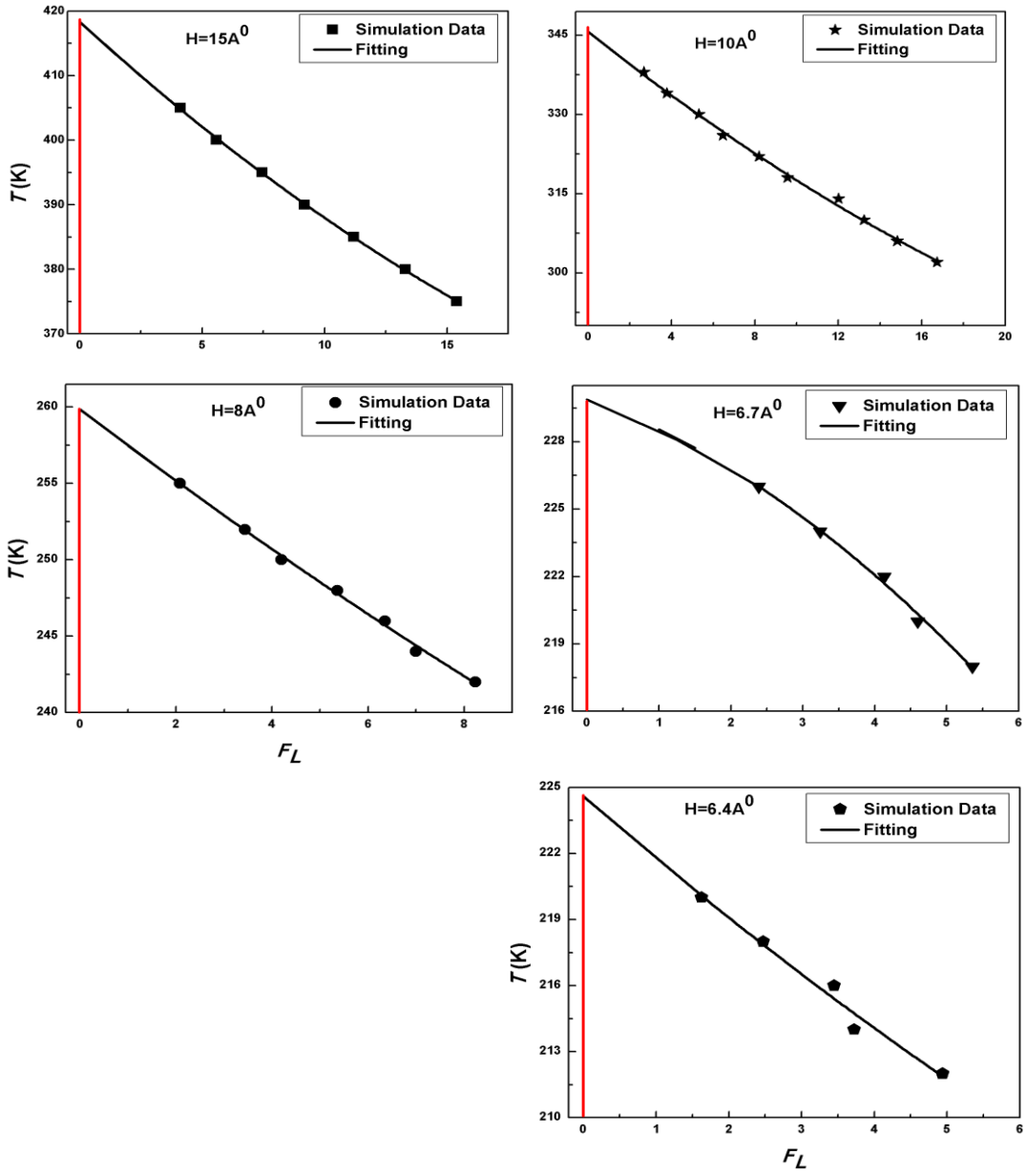

Figure 4.13(b). Temperature, T, vs. non-dimensional vapour-liquid interfacial free energy $F_L = (\beta F_L)$ is plotted and fitted with second degree polynomial for octane confined in mica slit pore.

The vapour- liquid free energy data, F_L, obtained in various cases are fitted with the second-degree polynomial to get the T corresponding to zero F_L, as depicted in Figure 4.13 (a) and 4.13 (b).

4.14 Critical temperature of bulk and confined octane and corresponding fitting parameters

The T(K) corresponding to zero F_L is estimated critical temperature, T_c. The values of fitting parameters A, B and C for the studies cases are reported in Table 5. The estimated critical temperatures, T_c, using this technique are reported in the following table.

Table 5. Critical temperature, T_c of bulk and confined n-octane a) Graphite-octane b) Mica-octane for various slit width, H is tabulated. The system volume, V, considered in each simulation is also included. The corresponding second-degree polynomial fitting parameters A, B and C are also included.

- Polynomial fitting of interfacial free energy, F_L :
- Formula used: $T = A + BF_L + CF_L^2; F_L = 0$ at T = T_c

Slit Width (H)	System Vol. (V) (Å^3)	A = T_c	B	C
Bulk	216000	545.03286±1.14612	-2.22731±0.12448	0.01724±0.00263
Graphite				
50	245000	519.70286±1.05339	-3.91408±0.24748	0.08383±0.0129
40	196000	511.19194±0.56032	-3.81096±0.14191	0.07074±0.00777
30	147000	494.5686±0.59793	-3.52298±0.08637	0.03919±0.00271
20	128000	459.45838±2.61399	-4.54365±0.48924	0.08042±0.02192
15	121500	406.60694±0.59541	-4.3263±0.19516	0.08389±0.01425
12	172800	352.79737±1.68877	-1.96541±0.46985	-0.01447±0.02921
10	81000	268.76189±7.93596	-1.97968±2.03301	-0.03067±0.12706
9	129600	248.0829±1.38224	-1.51751±0.43285	-0.04775±0.03127
8	115200	230.40314±1.25053	-2.46363±0.47725	0.03931±0.04137
7	100800	211.43391±16.54947	-9.32064±7.35865	0.82568±0.77418
Mica				
50	245000	508.30508±0.87144	-3.3873±0.17374	0.04156±0.00761
40	196000	497.98757±6.81496	-3.74085±1.51008	0.0536±0.07681
30	147000	484.7617±1.05823	-4.729±0.24278	0.09147±0.01148
20	128000	457.24841±6.89152	-5.23293±1.62989	0.1316±0.09273
15	121500	418.28035±0.66616	-3.45067±0.1517	0.04209±0.0077
10	81000	345.65491±0.99504	-3.14557±0.23947	0.03309±0.01225
8	115200	259.83916±0.78681	-2.38849±0.33151	0.02593±0.03165
7	100800	247.71793±15.25364	-6.51206±8.72354	0.47754±1.20718
6.7	96480	229.87524±2.2267	-1.12925±1.21351	-0.20568±0.15645
6.5	93600	224.60504±2.5209	-2.87769±1.6528	0.06127±0.24965

4.15 Comparison of the estimated critical temperature of bulk and confined octane using two different methods

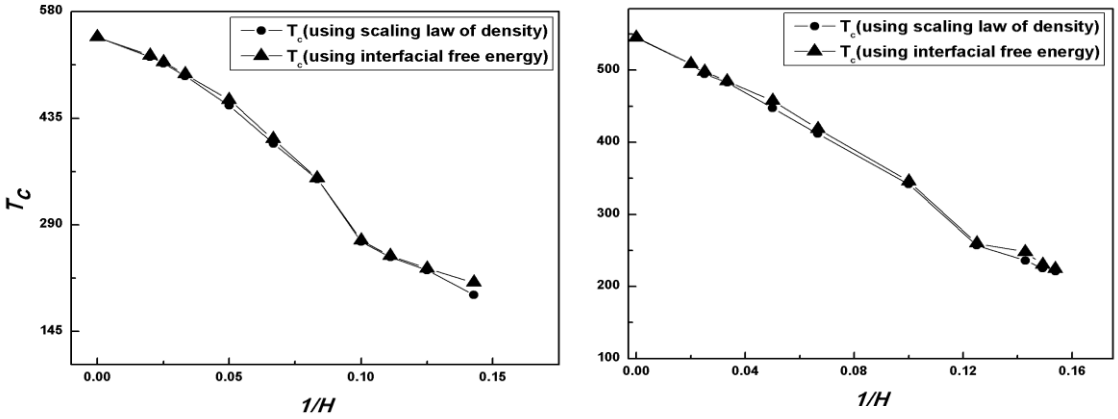

a) Graphite-octane b) Mica-octane

Figure 4.15. Dependence of critical temperature, T_c on the inverse slit width (1/H) is shown for investigated Confined n-octane a) Graphite-octane b) Mica-octane and compared with that obtained using simplified form of scaling law.

The estimated T_c for bulk and confined n-octane is further compared with the T_c estimated using simplified from scaling law[5] and the comparison is shown in the Table 6 and in Figure 4.15. It can be seen that the T_c estimated using both the techniques follow the same trend for bulk and the confined n-octane (Graphite-octane and Mica-octane) H (Å) = 50, 40, 30, 20, 15, 12, 10, 9, 8, 7 and H (Å) = 50, 40, 30, 20, 15, 10, 8, 7, 6.7, 6.5 respectively. Moreover, T_c estimated using F_L is lower by, 0.1 K, 1.5 K, 1.7 K, 2.3 K, 7.3 K, 6.4 K, 0.4 K, 1.6 K, 2.1 K, 2.1 K, 16.7 K, 0.1 K, 0.02 K, 3.1 K, 1.9 K, 9.6 K, 6.6 K, 4.1 K, 2.6 K, 11.7 K and 4.5 K than the T_c estimated using simplified form of scaling law, for the studied bulk and confined n-octane. This clearly shows insignificant difference in the estimated T_c's using the above two techniques.

Table 6. Comparison of the estimated critical temperature, T_c of bulk and confined n-octane (Graphite-octane and Mica-octane) using two different methods is tabulated.

Slit Width (H)	1/H	Scaling Law (T_c) K	Interfacial Free Energy (T_c) K
Bulk	0	545.19	545.03286
Graphite			
50	0.02	518.18	519.70286
40	0.025	509.434	511.19194
30	0.03333	492.22	494.5686
20	0.05	452.088	459.45838
15	0.06667	400.11	406.60694
12	0.08333	352.35	352.79737
10	0.1	267.13	268.76189
9	0.11111	245.9	248.0829
8	0.125	228.3	230.40314
7	0.14286	194.7	211.43391
Mica			
50	0.02	545.19	545.03286
40	0.025	508.28	508.30508
30	0.03333	494.831	497.98757
20	0.05	482.767	484.7617
15	0.06667	447.6	457.24841
10	0.1	411.63	418.28035
8	0.125	341.548	345.65491
7	0.14286	257.149	259.83916
6.7	0.14925	235.985	247.71793
6.5	0.15385	225.3141	229.87524

In Figure 4.15, comparison of the critical temperature, T_c estimated by the two methods, is shown with respect to inverse of the slit width, h. In this Figure, T_c estimation is compared using the simplified form of scaling law of density[5] and the T_c estimated corresponding to zero interfacial free energy, F_L. In the Figure 4.15, T_c of bulk system is also included, which is the case corresponding to 1/H = 0. Moreover, Figure 4.15 shows interesting monotonic decreasing behaviour of T_c with respect to inverse H, irrespective

of techniques used to estimate the T_c. Further, with decrease in the slit width, H, the critical temperature T_c decreases monotonically until H = 8 Å for confined graphite-octane and for confined mica-octane H = 6.7 Å; however, for confined graphite-octane $8 < H \leq 7$ and for confined mica-octane $6.7 < H \leq 6.5$, T_c becomes approximately indifferent with change in H. This behaviour primarily indicates significant differences in structural properties of vapour and liquid like phases in various regimes of slit width, as described in the earlier work. These regimes have different slopes, which indicate that the rate of change in T_c is not constant across the studied slit width range. Moreover, simplified form of scaling law[5] indicates that the difference in the coexistence vapour and liquid densities ($\rho l - \rho v$) plays major role in the estimated T_c. The coexistence vapour and liquid densities are the average outcomes of the local structural behaviour of the coexisting phases under confinement. This in turn indicates that the structural changes in fluid phases with degree of confinement play a significant role in their respective average coexistence densities and, hence, on the critical temperature, T_c, as depicted in the earlier work. Interestingly, it is observed that T_c remains indifferent for $H < 8$ for confined graphite-octane and $H < 6.7$ for confined mica-octane. On the major reason of this beaviour of T_c is that the maximum possible layer in local structural behaviour is limited to one for $H < 8$ for confined graphite-octane and $H < 5.7$ for confined mica-octane. Therefore, the difference in coexistence densities, ($\rho l - \rho v$) becomes approximately indifferent in the extremely small pores and so does the T_c, which eventually approaches to the two- value at H = 7 Å for confined graphite-octane and H = 6.5 Å for confined mica-octane. Moreover, the maximum difference in tc estimated corresponding to the zero F_L and that estimated using the simplified form of the scaling law[5] is less than 1% for the bulk and for confined graphite-octane with $50 \leq H \leq 30$; for confined mica-octane $50 \leq H \leq 30$. Whereas, for the studies with $30 \leq H \leq 7$ for confined graphite-octane, $30 \leq H \leq 6.5$ for confined mica-octane, the maximum differences in the estimation Tc using two techniques is less than 3%.

Chapter 5

Conclusions

We investigate, in this work, the critical temperature of bulk and confined Alkanes using vapour-liquid interfacial free energy values of phase coexistence obtained from the GC-TMMC simulation and histogram reweighting technique. For a system under investigation, the free energy data are estimated for a specified system volume and various temperature in a proper range. The coexistence interfacial free energy values fitted with the second-degree polynomial to estimate the temperature consequent to zero interfacial free energy. The estimated critical temperature under confinement is originated to decrease monotonically with decreasing slit width and also compared with the critical temperature obtained using simplified form of scaling law. The observed trend of critical temperature estimation with inverse of slit width is approximately same from both estimations (i.e, using scaling law of density and interfacial free energy). This in turn indicates that critical temperature using vapour-liquid interfacial free energy values at coexistence is in logically good agreement with that obtained using simplified form of scaling law. In this work, critical temperature of confined methane, n-butane & n-octane are studied in graphite and mica slit pores of varying pore width & also compared with the corresponding bulk values. Moreover, our investigation indicates that the surface characteristics and the extent of confinement affect significantly the critical temperature of n-alkanes. The critical temperature decreases constantly up to a certain minimum slit width, and then it becomes constant as the system approaches the two-dimensional regime.

Chapter-6

6. References

1. Binder, K., Critical Properties from Monte Carlo Coarse Graining and Renormalization. *Phys. Rev. Lett.* **1981,** *47*, 693-696.

2. Rżysko, W.; Patrykiejew, A.; Sokolowski, S.; Pizio, O., Phase behavior of a two-dimensional and confined in slitlike pores square-shoulder, square-well fluid. *J. Chem. Phys.* **2010,** *132*, 164702-164712.

3. Rzysko, W.; Borowko, M., A critical behavior of the Lennard–Jones dimeric fluid in two-dimensions.: A Monte Carlo study. *Surface Science* **2011,** *605*, 1219-1223.

4. Singh, S. K.; Singh, J. K., A comparative study of critical temperature estimation of atomic fluid and chain molecules using fourth-order Binder cumulant and simplified scaling laws. *Molecular Simulation* **2013,** *39*, 154-159.

5. Singh, S. K.; Saha, A. K.; Singh, J. K., Molecular Simulation Study of Vapor-Liquid Critical Properties of a Simple Fluid in Attractive Slit Pores: Crossover from 3D to 2D. *J. Phys. Chem. B* **2010,** *114*, 4283-4292.

6. Wegner, F., Corrections to Scaling Laws. *Phys. Rev. B.* **1972,** *5*, 4529-4536.

7. Singh, S. K.; Sinha, A.; Deo, G.; Singh, J. K., Vapor-Liquid Phase Coexistence, Critical Properties, and Surface Tension of Confined Alkanes. *J. Phys. Chem. C* **2009,** *113*, 7170-7180.

8. Singh, J. K.; Adhikari, J.; Kwak, S. K., Vapor–liquid phase coexistence curves for Morse fluids. *Fluid. Phase. Equil.* **2006,** *248*, 1-6.

9. Liu, Y.; Panagiotopoulos, A. Z.; Debenedetti, P. G., Finite-size scaling study of the vapor-liquid critical properties of confined fluids: Crossover from three dimensions to two dimensions. *J. Chem. Phys.* **2010,** *132*, 144107-144116.

10. Wilding, N. B., Critical-point and coexistence-curve properties of the Lennard-Jones fluid: A finite-size scaling study. *Phys. Rev. E* **1995,** *52*, 602-611.

11. Caillol, J. M., Critical-point of the Lennard-Jones fluid: A finite-size scaling study. *J. Chem. Phys.* **1998,** *109*, 4885-4893.

12. Errington, J. R., Direct calculation of liquid–vapor phase equilibria from transition matrix Monte Carlo simulation. *J. Chem. Phys.* **2003,** *118*, 9915-9925

13. Errington, J. R., Evaluating surface tension using grand-canonical transition-matrix Monte Carlo simulation and finite-size scaling. *Phys. Rev. E* **2003,** *67*, 012102.

14. Gupta, S. A.; Cochran, H. D.; Cummings, P. T., Shear behavior of squalane and tetracosane under extreme confinement. II. Confined film structure. *J. Chem. Phys.* **1997,** *107*, 10327-10334.

15. Bhatia S., Adsorption of Binary Hydrocarbon Mixtures in Carbon Slit Pores: A Density Functional Theory Study. *Langmuir* **1998,** *14*, 6231-6240.

16. Altwasser S.; Welker C.; Traa Y.; Weitkamp J., Catalytic cracking of n-octane on small-pore zeolites. *Microporous Mesoporous Mater.* **2005,** *83*, 345-356.

17. Gelb, L. D.; Gubbins, K. E.; Radhakrishnan, R.; Sliwinska-Bartkowiak, M., Phase separation in confined systems. *Rep. Prog. Phys.* **1999,** *62*, 1573-1659.

18. Machin, W. D., Temperature Dependence of Hysteresis and the Pore Size Distributions of Two Mesoporous Adsorbents. *Langmuir* **1994,** *10*, 1235-1240.

19. Wong, A. P. Y.; Kim, S. B.; Goldburg, W. I.; Chan, M. H. W., Phase separation, density fluctuation, and critical dynamics of N2 in aerogel. *Phys. Rev. Lett.* **1993,** *70*, 954-957.

20. Thommes, M.; Findenegg, G. H., Pore condensation and critical-point shift of a fluid in controlled-pore glass. *Langmuir* **1994,** *10*, 4270-4277.

21. Morishige K.; Shikimi M., Adsorption hysteresis and pore critical temperature in a single cylindrical pore. *J. Chem. Phys.* **1998,** *108*, 7821-7830.

22. Zhang, X.; Wang, W., Square-well fluids in confined space with discretely attractive wall-fluid potentials: Critical point shift. *Phys. ReV. E* **2006,** *74*, 062601-1-062601-4.

23. Vishnyakov, A.; Piotrovskaya, E. M.; Brodskaya, E. N.; Votyakov, E. V.; Tovbin, Y. K., Critical Properties of Lennard-Jones Fluids in Narrow Slit-Shaped Pores. *Langmuir* **2001,** *17*, 4451-4458.

24. Vörtler, H. L., Vapor-liquid critical and interfacial properties of square-well fluids in slit pore. *Collect. Czech. Chem. Commun.* **2008,** *73*, 518-532.

25. Vörtler, H. L.; Smith, W. R., Computer simulation studies of a square-well fluid in a slit pore. Spreading pressure and vapor–liquid phase equilibria using the virtual-parameter-variation method. *The Journal of Chemical Physics* **2000,** *112* (11), 5168-5174.

26. Kofke, D. A., Gibbs-Duhem integration: a new method for direct evaluation of phase coexistence by molecular simulation. *Molecular Physics* **1993,** *78* (6), 1331-1336.

27. Moller, D.; Fischer, J., Vapour liquid equilibrium of a pure fluid from test particle method in combination with NpT molecular dynamics simulations. *Mol. Phys.* **1990,** *69* (3), 463-473.

28. Lofti, A.; Vrabec, J.; Fischer, J., Vapour liquid equilibria of the Lennard-Jones fluid from the NpT plus test particle method. *Mol. Phys.* **1992,** *76* (6), 1319-1333.

29. Sarkisov, L.; Monson, P. A., Computer simulations of phase equilibrium for a fluid confined in a disordered porous structure. *Phys. Rev. E* **2000,** *61* (6), 7231-7234.

30. (a) Forsman, J.; Woodward, C. E., Simulations of phase equilibria in planar slits. *Mol. Phys.* **1997,** *90* (4), 637-652; (b) Singh, S. K., Effect of surface-screening parameter of the Yukawa potential model on vapour–liquid phase coexistence and critical-point properties of confined Yukawa fluid. *Molecular Simulation* **2016,** *42* (5), 413-419.

31. Singh, S. K.; Singh, J. K., Effect of pore morphology on vapor–liquid phase transition and crossover behavior of critical properties from 3D to 2D. *Fluid Phase Equilib.* **2011,** *300*, 182-187.

32. Vörtler, H. L.; Schäfer, K.; Smith, W. R., Simulation of chemical potentials and phase equilibria in two-and three-dimensional square-well fluids: finite size effects. *The Journal of Physical Chemistry B* **2008,** *112* (15), 4656-4661.

33. Panagiotopoulos, A. Z., Direct determination of phase coexistence properties of fluids by Monte Carlo simulation in a new ensemble. *Mol. Phys.* **1987,** *61*, 813-826.

34. Pe´rez-Pellitero, J.; Ungerer, P.; Mackie, A. D., Effective critical point location: application to thiophenes. *Molecular Simulation* **2007,** *33*, 777-785.

35. Gelb L. D.; Gubbins K. E.; Radhakrishnan R.; Sliwinska-Bartkowiak M., Phase separation in confined systems. *Rep. Prog. Phys.* **1999,** *62*, 1573–1659.

36. Bhatia, S. K., Adsorption of Binary Hydrocarbon Mixtures in Carbon Slit Pores: A Density Functional Theory Study. *Langmuir* **1998,** *14*, 6231–6240.

37. Binder, K.; Landau, D.; Müller, M., Monte Carlo Studies of Wetting, Interface Localization and Capillary Condensation. *J. Stat. Phys.* **2003,** *110*, 1411-1514.

38. Jiang, J. W.; Sandler, S. I., Adsorption and phase transitions on nanoporous carbonaceous materials: insights from molecular simulations. *Fluid Phase Equilibria* **2005,** *228*, 189-195.

39. Jiang, J. W.; Sandler, S. I.; Schenk, M.; Smit, B., Adsorption and separation of linear and branched alkanes on carbon nanotube bundles from configurational-bias Monte Carlo simulation. *Phys. Rev. B* **2005,** *72*, 045447-1-045447-11.

40. Zhang, F., Molecular dynamics studies of chainlike molecules confined in a carbon nanotube. *J. Chem. Phys.* **1999,** *111*, 9082-9085.

41. Do, D. D.; Do, H. D., Evaluation of 1-Site and 5-Site Models of Methane on Its Adsorption on Graphite and in Graphitic Slit Pores. *J. Phys. Chem. B* **2005,** *109*, 19288–19295.

42. Kowalczyk, P.; Tanaka, H.; Kaneko, K.; Terzyk, A. P.; Do, D. D., Grand Canonical Monte Carlo Simulation Study of Methane Adsorption at an Open Graphite Surface and in Slitlike Carbon Pores at 273 K. *Langmuir* **2005,** *21*, 5639–5646.

43. Vishnyakov, A.; Piotrovskaya, E. M.; Brodskaya, E. N., Monte Carlo Computer Simulation of Adsorption of Diatomic Fluids in Slitlike Pores. *Langmuir* **1996,** *12*, 3643–3649.

44. Klochko, V. A.; Brodskaya, E. N.; Piotrovskaya, E. M., Computer Simulations of Dependence of Adsorption Characteristics of Ethane on the Size of Graphite Micropores. *Langmuir* **1999,** *15*, 545–552.

45. Calleja, G.; B., C.; Pinar, A.; Morales-Cas, A. M., Ethane adsorption in slit-shaped micropores: influence of molecule orientation on adsorption capacity. *Adsorption* **2006,** *12*, 45-54.

46. Do, D. D.; Do, H. D., Adsorption of flexible n-alkane on graphitized thermal carbon black: analysis of adsorption isotherm by means of GCMC simulation. *Chem. Eng. Sci.* **2005,** *60*, 1977-1986.

47. Severson, B. L.; Snurr, R. Q., Monte Carlo simulation of n-alkane adsorption isotherms in carbon slit pores. *J. Chem. Phys.* **2007,** *126*, 134708-1-134708-7.

48. Balasundaram, R.; Jiang, S. Y.; Belak, J., Structural and rheological properties of n-decane confined between graphite surfaces. *Chem. Eng. J.* **1999,** *74*, 117-127.

49. Wang, J. C.; Fichthorn, K. A., Influence of molecular structure on the properties of confined fluids by molecular dynamics simulation. *Colloids and Surfaces A* **2002,** *206*, 267-276.

50. Cui, S. T.; Gupta, S. A.; Cummings, P. T.; Cochran, H. D., Molecular dynamics simulations of the rheology of normal decane, hexadecane, and tetracosane. *J. Chem. Phys.* **1996,** *105*, 1214-1220.

51. Cui, S. T.; Cummings, P. T.; Cochran, H. D.; Moore, J. D.; Gupta, S. A., Nonequilibrium Molecular Dynamics Simulation of the Rheology of Linear and Branched Alkanes. *Int. J. Thermophys.* **1998,** *19*, 449–459.

52. Martini, A.; Liu, Y.; Snurr, R. Q.; Wang, Q. J., Molecular dynamics characterization of thin film viscosity for EHL simulation. *Tribol. Lett.* **2006,** *21*, 217–225.

53. Paluch, A. S.; Shen, V. K.; Errington, J. R., Comparing the Use of Gibbs Ensemble and Grand-Canonical Transition-Matrix Monte Carlo Methods to Determine Phase Equilibria. *Ind. Eng. Chem. Res.* **2008,** *47*, 4533-4541.

54. Berg, B. A.; Neuhaus, T., Multicanonical ensemble: A new approach to simulate first-order phase transitions. *Phys. Rev. Lett.* **1992,** *68* (1), 9-12.

55. Ferrenberg, A. M.; Swendsen, R. H., New Monte Carlo technique for studying phase transitions. *Phys. Rev. Lett* **1988,** *61*, 2635-2638.

56. Singh, J. K.; Kwak, S. K., Surface tension and vapor-liquid phase coexistence of confined square-well fluid. *J. Chem. Phys.* **2007,** *126*, 24702-24709.

57. Goujon, F. M.; Boutin, A.; Fuchs, A. H., Direct Monte Carlo simulations of the equilibrium properties of n-pentane liquid–vapor interface. *J. Chem. Phys.* **2002,** *116*, 8106 - 8117.

58. Ryckaert, J. P.; Bellemans, A., Molecular dynamics of liquid n-butane near its boiling point. *CHemical Physics Letters* **1975,** *30*, 123-125.

59. Errington, J. R.; Panagiotopoulos, A. Z., A New Intermolecular Potential Model for the n-Alkane Homologous Series. *J. Phys. Chem. B* **1999,** *103*, 6314–6322.

60. Steele, W. A., The physical interaction of gases with crystalline solids: I. Gas-solid energies and properties of isolated adsorbed atoms. *Surf. Sci.* **1973,** *36*, 317-352.

61. Siepmann, J. I.; Frenkel, D., Configurational bias Monte Carlo: a new sampling scheme for flexible chains. *Molecular Physics* **1992,** *75*, 59-70.

62. de Pablo, J. J.; Laso, M.; Suter, U. W., Simulation of polyethylene above and below the melting point. *J. Chem. Phys.* **1992,** *96*, 2395-2403.

63. Errington J. R., Direct calculation of liquid–vapor phase equilibria from transition matrix Monte Carlo simulation. *J. Chem. Phys.* **2003,** *118*, 9915-9925

64. Errington, J. R., Evaluating surface tension using grand-canonical transition-matrix Monte Carlo simulation and finite-size scaling. *Phys. Rev. E* **2003,** *67*, 012102-1:012102-4.

65. Berg, B. A.; Nneuhaus, T., Multicanonical ensemble: A new approach to simulate first-order phase transitions. *Phys. Rev. Lett.* **1992,** *68*, 9-12.

66. Fitzgerald, M.; Picard, R. R.; Silver, R. N., Canonical transition probabilities for adaptive Metropolis simulation. *Europhys. Lett.* **1999,** *46*, 282-287.

67. Fitzgerald, M.; Picard, R. R.; Silver, R. N., Monte Carlo Transition Dynamics and Variance Reduction. *J. Stat. Phys.* **2000,** *98*, 321–345

68. Ferrenberg, A. M.; Swendsen, R. H., New Monte Carlo technique for studying phase transitions. *Phys. Rev. Lett.* **1988,** *61*, 2635-2638.